International Journal of Nanomedicine

Dovepress
open access to scientific and medical research

Open Access Full Text Article

ORIGINAL RESEARCH

Nanobubble Ozone Stored in Hyaluronic Acid Decorated Liposomes: Antibacterial, Anti-SARS-CoV-2 Effect and Biocompatibility Tests

Ahmet Umit Sabancı [1,*]
Perihan Erkan Alkan [2,*]
Cem Mujde [3,*]
Hivda Ulbeği Polat [4,*]
Cemre Ornek Erguzeloglu [5,*]
Atil Bisgin [3,6,*]
Cuneyt Ozakin [7,*]
Sehime G Temel [5,8,9,*]

[1]Bursa Çekirge State Hospital, Orthopedics and Traumatology Clinic, Bursa, Turkey; [2]Bursa Uludağ University, Vocational School of Health Services, Medical Laboratory Technician Department, Bursa, Turkey; [3]Çukurova University AGENTEM (Adana Genetic Diseases and Treatment Center), Adana, Turkey; [4]TUBITAK, Marmara Research Center, Genetic Engineering and Biotechnology Institute, Gebze, Kocaeli, Turkey; [5]Bursa Uludag University, Institute of Health Sciences, Department of Translational Medicine, Bursa, Turkey; [6]Çukurova University, Faculty of Medicine, Department of Medical Genetics, Adana, Turkey; [7]Bursa Uludağ University, Faculty of Medicine, Department of Infectious Diseases and Microbiology, Bursa, Turkey; [8]Bursa Uludağ University, Faculty of Medicine, Department of Medical Genetics, Bursa, Turkey; [9]Bursa Uludag University, Health Sciences Institute, Department of Translational Medicine, Bursa, Turkey

*These authors contributed equally to this work

Purpose: SARS-CoV-2-infected individuals may be asymptomatic, and therefore, the virus is highly contagious. We aimed to develop an agent to control viral replication in the upper respiratory tract and to prevent progression of the disease into the lower airways as well as inter-individual transmission. For this purpose, we investigated the antibacterial and antiviral activities of our novel nanobubble ozonated hyaluronic acid-decorated liposomal (NOHAL) solution, developed by using nanotechnology.

Methods: The MIC levels of NOHAL solution were determined on blood agar cultures of *Staphylococcus aureus* (ATCC 6538), *Streptococcuspneumoniae* (ATCC 49619) and *Escherichia coli* (ATCC 25922). The in vitro anti-viral activity of NOHAL solution was studied using recombinant SARS-CoV-2 copies of the original virus, grown in Vero cells generated by reverse genetic technology. Human primary lung epithelial cells obtained by bronchoscopy or lung resection were used for cell viability tests using flow cytometry analysis. The cytotoxicity testing was performed using the BALB/c 3T3 (CCL-163) cell line. Skin, oral, nasal and ocular irritation tests were performed using New Zealand albino rabbits, Syrian hamsters, BALB c mice and New Zealand albino rabbits of both sexes.

Results: Bacterial growth was prevented by NOHAL solution in a time-/dose-dependent manner. In vivo or in vitro experiments did not show any toxicity of NOHAL solution. No cytotoxicity was recorded on cell viability. No skin, oral, nasal or ocular toxicities were recorded. In addition, in a SARS-CoV-2 mouse infection model, NOHAL solution diminished the viral RNA levels effectively in nasopharyngeal and lung samples after its prophylactic intranasal application.

Conclusion: NOHAL solution has the potential to reduce or prevent the spread of SARS-CoV-2 through the nose and/or oral cavity. The clinical efficacy of this solution needs to be tested in order to determine its efficacy in the early phase of COVID-19.

Keywords: nanobubble, ozone, hyaluronic acid, liposome, anti-microbial, anti-viral

Correspondence: Cuneyt Ozakin
Bursa Uludağ University, Faculty of Medicine, Department of Infectious Diseases and Microbiology, Bursa, Turkey
Email ozakin@uludag.edu.tr

Sehime G Temel
Bursa Uludağ University, Faculty of Medicine, Department of Medical Genetics, Bursa, Turkey
Email sehime@uludag.edu.tr

Introduction

After fluorine and persulfate, ozone (O_3) is the third strongest oxidizing agent, and a highly reactive molecule.[1] It is the allotropic form of oxygen and is used in a number of applications in scientific, medical, and industrial fields. O_3 is a trophic agent that has analgesic, anti-inflammatory and immunomodulatory properties,[2] and has been used in complementary medicine to treat various infectious as well as autoimmune and degenerative disorders.[3]

Received: 10 July 2021
Accepted: 24 December 2021
Published: 25 January 2022

Today, ozone is increasingly used as a therapeutic agent. A number of studies from different countries including China, Italy, Turkey, Russia and Spain have reported the use of O_3 in many conditions.[4–9] It has been reported that O_3 can reduce inflammation and pain[6,8,9,10] and show bactericidal,[11] fungicidal,[12] virucidal[13] and antiparasitic effects.[14] O_3 is a potent oxidizing agent that is able to react with unsaturated triacylglycerides. In 1975, Criegee was the first to claim that O_3 exerted its action by cleaving double bonds by oxidation, and this has been widely accepted since then.[15] Ozonated vegetable oils have been successfully applied as complementary anti-infective,-[16] anti-inflammatory,[17] and wound-healing agents.[18]

Recently, Murata Takayuki and his colleagues showed the efficacy and safety of low-dose O_3 gas and O_3 water for SARS-CoV2 in an in vitro study.[19] On the other hand, in several studies, it was reported that O_2-O_3 therapy might be applied as an adjuvant to the available SARS-CoV-2 treatment methods, because it improved clinical outcomes, and was promising for COVID-19 patients.[19–23] Ozone has many beneficial properties that can also be useful in the treatment of COVID-19 pneumonia. It can provide sufficient energy and oxygen to the tissues by activating the pentose phosphate pathway, increasing the 2.3 diphosphoglyceric acid content in erythrocytes, and stimulating erythrocyte oxygen metabolism.[24–27] ,Moreover, its ability to improve blood rheology and capillary action has also been reported, which has been shown to be beneficial in the treatment of some vascular diseases. The antiplatelet effect of ozone increases the release of some prostacyclins such as PGI2, which is beneficial for patients with microthrombosis.[28] All these effects may help reduce the hypercoagulation phenomenon in the COVID-19 patients. The immunomodulatory effects of ozone may also play an important role in COVID-19.[29] An inflammatory response develops in response to the severe infection, and worsening of the general condition of the patient may be prevented by cytokine modulation. Ozone has strong anti-inflammatory features.[24–29]

O_3 has antiviral effects, and exerts this effect by interfering with the virus replication stage. The antiviral property of O_3 has been linked to the oxidization of cysteine residues. Like all other coronaviruses, SARS-CoV-2 is also rich in these residues, and O_3 oxidizes them to form disulfide bridges.

It has been reported that O_3 can directly inactivate various viruses including Norwalk, Hepatitis A and polio viruses.[30–34] Rowen stated that ozone oxidized the membrane glycoprotein, transforming it from the reduced form to the oxidized form. In this case, viruses cannot enter the cell and infect the host since they need the reduced form of membrane glycoproteins.[35]

Mirazmi et al observed that CMV (cytomegalovirus) loses its infective capacity if its "thiol" group is oxidized.[36] It was also reported that HIV needs reduced sulfhydryl groups for infectivity,[37] and the Ebola virus needs them to enter into cells.[38]

Similarly, Rowen postulated that thiol groups of cysteine and tryptophan could be directly oxidized by ozone, inactivating cellular fusion of the virus. In cases where the ozone molecule cannot directly reach the viral capsid, its mediators such as reactive oxygen species (ROS), including O_2, -OH, and H_2O_2 that are generated after decomposition of ozone, or lipid oxidation products (LOP) continue to maintain the oxidizing power required to inactivate the virus.[35] Moreover, the reactions between ozone and ozone-related ROS with the viral proteins, lipids and amino acids may cause the formation of further ROS, including acylperoxyl, promoting more oxidation via a chain reaction.

When the ozone molecule damages viral capsid through peroxidation, virus replication cycle is altered, meaning that the O_3 has a therapeutic effect at the initial phase of the viral infection. The coronavirus has been named after its crown-shaped S-spike protein, comprised of cysteine and tryptophan. O_3 or its mediators (LOP/ROS) are able to oxidize these amino acids, and prevent binding of coronavirus to the ACE2 receptors of Type 2 pneumocytes.[39]

Conventional molecule delivery systems have several known limitations. However, the nano-technological delivery systems have key advantages including the small size of the carrier, targetable, biocompatible and biodegradable features, less toxicity, delivery of molecules to specific regions thanks to the ability for surface modification, support in the long cycling time, and they also provide stability to the molecules, particularly medicines, surrounded by the nanotechnological carriers. Lipid sacs called liposomes/nanoliposomes are relatively new technological products used for encapsulating bioactive substances and delivering them to a specific target. The list of bioactive materials that can be delivered through these liposomes is quite long. Liposomes/nanoliposomes can improve the solubility and biocompatibility performance of the bioactive materials by maintaining their stability and preventing their nonspecific interactions with foreign molecules. Targeting ability is another advantage of these liposomes; they may be targeted to a specific region or cell, minimizing side

effects on healthy tissues and cells, as well as providing optimum therapeutic efficacy in the target. pH-sensitive liposomes are useful as intracellular drug cargo systems owing to their capability to transfer their contents into the cell through fusion or destabilization of the endosome with a weak acidic environment.[40–42]

In line with the aforementioned literature data in this study, Hyaluronic Acid (HA)-decorated ozonated nanoliposomes were developed to test the in vitro antibacterial and in vitro/in vivo antiviral (SARS-CoV-2) and toxicity effects of the ozone molecule. For this purpose, this molecule was encapsulated in nano-carrier oil with glycerin, HA, menthol and water, in a nanoscale manner. HA-modified ozonated nanoliposomes were used to deliver the ozone molecule to the target, which is the most effective way of increasing its therapeutic effect.

Materials and Methods

Animals and Mesenchymal Cell Line

All experimental procedures involving use of the animals were approved by the Akdeniz University, Committee for Animal Care and Use (B.30.2.AKD.0.05.07.00/141), carried according to the Animal Experiments Local Ethics Committee (Akhadyek) Establishment and Procedure Guideline, and TUBITAK HADYEK (16563500-111-88). Ethical approval for mesenchymal stem cells was obtained from the Non-invasive Clinical Studies Ethics Committee, Cukurova University Faculty of Medicine (31/08/2018-80-07).

Preparation of Solutions

In our study, the amount of ozonation of the liposome solutions was calculated in terms of ppm. Preparation of NOHAL is described and protected by patent applications (Patent application number TR201904790A·2019-03-29, US2021007360A1; WO2019240713A2; WO2019240713A3, TR2021-00105).

Size polydispersity (PDI), zeta potential, hydrodynamic diameter (Z-average size), and dynamic light scattering (DLS), (Electrophoretic Light Scattering/ELS) measurements were done at 25°C on three independent samples with a Zetasizer Nano ZS instrument (Malvern Instruments Ltd., UK) containing a solid-state HeNe laser (λ=633nm) at a 173° scattering angle.

In vitro Anti-Microbial Activity of NOHAL Solution

Determination of the Minimum Inhibitory Concentration (MIC) of Ozone Solutions

The CLSI M07 A9 method (Dilution Antimicrobial Sensitivity Tests for Aerobically Growing Bacteria) was used for antibacterial tests, performed in Medical Microbiology Department's Test Laboratory of Antimicrobial Efficiency (Approved Standard) (CLSI M07 A9)[43] in the Bursa Uludağ University, Faculty of Medicine. The proposed standard test method was employed for the antibacterial tests, and the MIC levels of NOHAL solution were determined using *Staphylococcus aureus* (ATCC 6538), *Streptococcus pneumoniae* (ATCC 49619) and *Escherichia coli* (ATCC 25922) (Table 1). First, a stock solution of ozone containing 50,000 ppm was prepared and serially diluted to 50,000, 25,000, 12,500, 6250, 3125, 1562, 780, 390, 195 and 97 ppm concentrations. The serial dilutions with the aforementioned concentrations were transported into sterile U tubes. 24-hour colonies of bacterial culture were used to obtain bacterial suspensions with a turbidity of 0.5 McFarland units, in accordance with CLSI (Institute of Clinical and Laboratory Standards) recommendations, and they were added to the ozone solutions in U tubes to obtain a final concentration of 3×10^6 colony forming units (CFU)/mL. This solution concentration in the tubes was set to initially proposed levels of 50,000, 25,000, 12,500,

Table 1 MIC Values for *Staphylococcus aureus* (ATCC 6538) and *Escherichia coli* (ATCC25922) According to the CLSI M07 A9 Method

	Tube	Dilution	ppm	*Staphylococcus aureus*	*Escherichia coli*
NOHAL	1	1	50.000	Absent	Absent
	2	2	25.000	Absent	Absent
	3	4	12.500	Absent	Absent
	4	8	6.250	Absent	Absent
	5	16	3.125	Absent	Absent
	6	32	1.562	Absent	Absent
	7	64	781	Present	Present
	8	128	390	Present	Present
	9	256	195	Present	Present
	10	512	97	Present	Present

6250, 3125, 1562, 780, 390, 195, 97 ppm. Then, the samples taken from the tubes using a standard cycle were cultivated in blood agar media (Germany-Becton Dickinson). The MIC value was defined as the lowest ozone concentration with no visible bacterial growth after incubation at 37 °C for 24 hours.

In vitro Anti-Viral Activity of NOHAL Solution

As Xie et al have shown, the replication kinetics of the isolates obtained from patients may be repeated by the recombinant virus generated by reverse genetic technology.[44] Thus, in our study, we used the recombinant SARS-CoV-2 replicates of the original virus grown in Vero cells (ATCC). African green monkey kidney-derived Vero cells were grown in DMEM (Dulbecco's Modified Eagle Medium, Sigma Aldrich, USA) added 5% FBS (fetal bovine serum). The cells were cultured at 37°C in a humidified 5% CO_2 incubator (ESCO, Singapore). Vero cells were transfected and grown on a Lab-Tek chamber slide with eight wells (Thermo Fisher Scientific, USA). The cell viability and RNA synthesis were monitored in transfected cells. RT-PCR was performed to detect the viral RNA, and flow cytometry was done to determine cell survival rates in the transfected Vero cells at indicated time points. The culture media of the transfected cells revealed SARS-CoV-2 RNA on RT-PCR; however, the cells transfected as negative controls did not yield any RT-PCR products. QIAamp Viral RNA Kits (QIAGEN, Germany) were used to extract viral RNA.

An in vitro analysis was performed to study the anti-SARS-CoV-2 activity of NOHAL solution. 96-well plates were used to seed the cells at a concentration of 1×10^4 cells per well, and growth was allowed for 24 hours. This experiment had four parts: (i) treatment with 300 ppm NOHAL solution, (ii) treatment with 600 ppm NOHAL solution, (iii) treatment with 1000 ppm NOHAL solution, (iv) treatment with 1600 ppm NOHAL solution, and (v) the study for prophylaxis.

The Vero cells were treated with NOHAL solution at different concentrations, ranging from 300 ppm to 1600 ppm, for 2, 12 and 24 hours, in the treatment groups in accordance with the previous studies of our group, previous ozone in vitro cytotoxicity assays and recent anti-SARS-CoV-2 effects of ozone therapies.[45–48] Exposure times for treatment were determined by following up the chronic effect, cytotoxicity and the impact on the cell proliferation. The maximum time was calculated in relation to the cells' doubling time. Each assay was performed twice. Statistical comparisons were made using the median values of the replicates. The Vero cells that were not treated with NOHAL solution were used as negative controls. Then, a medium containing recombinant SARS-CoV-2 replicates was added to the Vero cells treated with NOHAL and it remained for 2 hours. After removal of the medium, a fresh medium that contained neither the treatment content nor the virus-related ingredients was added. Next, RNA was extracted from the supernatant and analyzed using the previously published RT-PCR method.[49] Extraction of the viral RNA from the supernatant of infected cells (100 µL) was done with an automated nucleic acid extraction system (QiaSymphony, QIAGEN, Germany), following the instructions of the manufacturer.

One Step Prime Script RT-PCR kit (TaKaRa, Japan) was used on a Light Cycler 480 Real-Time PCR system (Roche, Rotkreuz, Switzerland) to detect SARS-CoV-2, using the primers with the following sequences: forward primer: 5′-AGAAGATTGGTTAGATGATGATAGT-3′; reverse primer: 5′-TTCCATCTCTAATTGAGGTTGAACC-3′; and probe: 5′-FAM-TCCTCACTGCCGTCTTGTTG ACCA-BHQ1-3′.

Human Cell Line Culture and Viability Test of NOHAL Solution

Human primary lung epithelial cells preserved in Cukurova University Cell and Biobank were used for cell viability tests. The cells were cultured in DMEM containing penicillin plus streptomycin 1%, L-glutamine 1% and FBS 10%.[50,51] Cell viability testing was performed via flow cytometry analysis. All samples' cell concentrations were higher than 1 x 10e4 cells/mL. Thus, 20 µL 7AAD (Beckman Coulter, USA) for every 1 mL of cells was directly added to the cells in the culture media. Then, all were mixed and read on the CytoFLEX cytometer (Beckman Coulter, USA) within 10 minutes.

Additionally, to eliminate subjectivity and user-to-user variability and to assess the infected cells, the samples were stained with Trypan Blue (100 µL with 0.4% concentration for each sample), and examined using a sophisticated image analysis system with an auto-focus mechanism (The Countess II Automated Cell Counter, ThermoFisher, USA).

The primary cells isolated from lung tissue were airway epithelial cells obtained with bronchoscopy or lung resection, and a commercial source (Lonza) was also utilized.[54,55] Lung tissues were obtained by bronchoscopy or lung resection under aseptic surgical conditions in order to isolate bronchial epithelial cells, and were brought to the laboratory in a sterile bucket. During transport and prior to dissection, tissue samples were preserved at 4 °C. The tissue samples were placed into a petri dish containing 2% Penicillin + Streptomycin PBS during the dissection, and then washed with PBS three times to eliminate blood residues. Dissected tissue was transferred into a sterile petri dish and minced with a lancet. Minced tissue was mixed with 10 mL PBS containing 1 mg/mL collagenase in a sterile 50 mL tube, and homogenized by shaking. After 1-hour incubation at 37 °C, the tube was centrifuged at 400xg for 5 minutes. After removal of the supernatant, the pellet was suspended again using 10 mL PBS. This step was repeated twice. After PBS was removed, 25 mL 0.25% Trypsin/EDTA was added into tube and mixed gently and left to incubate for 1 hour at 37 °C. After incubation, 1 mL fetal bovine serum (FBS) was added and the tube was centrifuged at 400xg for 5 minutes. Removal of the supernatant was followed by re-suspension of the pellet with 10 mL phosphate buffered saline (PBS), which was done twice. After the second wash, the supernatant was removed and 10 mL mesenchymal cell culture media was added (Dulbecco's Modified Eagle Medium, 10% FBS, 1% penicillin, streptomycin), and mixed through pipetting. The suspension was transferred into a T-75 flask and cultured in a humidified incubator with 5% CO_2 at 37 °C. After incubation for 48 hours, the medium was removed, and the flask was washed with culture medium. Then, 10 mL medium was added. The medium was changed every 72 hours. When the confluency reached 80–90%, cells were washed with 10 mL PBS twice, and then 5mL 0.25% Trypsin/EDTA was added and they were removed from the flask. It was then incubated for 5 minutes at 37 °C. After incubation, 10 mL culture media was added into the flask and mixed with pipetting. The suspension was transported into a 50 mL tube, centrifuged at 400xg for 5 minutes, aspirated and re-suspended with 10 mL fresh culture media. In order to count cells with a cell counter, 10 µL trypan blue was used to dilute 10 µL of cell suspension, and the total number of cells was calculated. The cells were then transferred to new flasks at 1150 cells/cm^2 in fresh cell culture media, and incubated in a tissue culture incubator (with 5% CO_2, at 37 °C). These cells were preserved in the biobank for further studies.

This cell culture procedure has a better physiological function compared to continuous cell lines, although their life span is limited. Both the isolation and culturing procedures including passaging were performed as reported in a previous study.[56] Moreover, to generate a 3-Dimensional (3-D) lung model, we used the rotary cell culture system (RCCS) as a bioreactor (Synthecon, USA) at 37°C under 5% CO_2. In order to generate the lung model, bronchial epithelial cells that were obtained from lung resection and bronchoscopy were cultured at 37°C in 5% CO_2 as 2-D in T-75 flasks with GTSF-2 medium (HyClone), by adding 10% FBS and 100 g of penicillin-streptomycin (Invitrogen). PBS was used to wash the cells twice after they reached 75% confluency, then 0.25% Trypsin/EDTA was added to remove them from the flask. After the cells were counted, around 5×10^6 cells were suspended again in fresh GTSF-2 that included 5 mg/mL Cytodex-3 microcarrier beads (Sigma). These beads were dextran beads coated with type I collagen- (mean diameter, 175µ). The cell-bead mixture was incubated at room temperature for 30 min to allow their attachment, and as previously reported, placed into the RCCS and cultured in GTSF-2. Before using them for studies, the RCCS bioreactor was used to culture 3-D aggregates for 12 to 14 days, then they were seeded on 24-well plates on the experimental day, and fresh medium was added. The cell monolayers were cultured for 2–3 days in GTSF-2 in 24-well plates to 75% confluency, under 5% CO_2 and at 37°C. Treatment studies were performed using these 3-D cultures grown for 12–16 days. The timelines for the Trypan Blue dye exclusion test were matched for each parallel testing to establish the number of viable cells in the cell culture.

Placenta Derived Mesenchymal Stem Cell Isolation Protocol

The placentas obtained under aseptic surgical conditions after Cesarean section were brought to the laboratory in a sterile bucket. The placentas were stored at 4°C while being transported and prior to dissection. The isolation steps were carried out as follows:

Chorionic villus tissue was dissected from placental tissue ~1 cm^2 × 0.5–1 cm deep. The tissue samples were placed into a petri dish containing 2% Penicillin + Streptomycin PBS during the dissection, and then

washed with PBS three times to eliminate blood residues.

Dissected tissue was transferred into a sterile petri dish to mince with a lancet. Minced tissue was mixed in a sterile 50 mL tube with 10 mL PBS that contained 1 mg/mL collagenase, and homogenized by shaking. After 1-hour incubation at 37°C, the tube was centrifuged at 400xg for 5 minutes. Removal of the supernatant was followed by re-suspension of the pellet with 10 mL PBS, which was repeated twice. After PBS was removed, 25 mL 0.25% Trypsin/EDTA was added into tube and mixed gently and left to incubate for 1 hour at 37 °C. After incubation, 1 mL fetal bovine serum (FBS) was added and the tube was centrifuged at 400xg for 5 minutes. After removal of the supernatant, 10 mL phosphate buffered saline (PBS) was used to re-suspend the pellet, which was repeated twice.

After the second wash, the supernatant was removed and 10 mL mesenchymal stem cell culture media was added (Dulbecco's Modified Eagle Medium, 10% FBS, 1% penicillin, streptomycin) and mixed through pipetting. The suspension was transferred into a T-75 flask and cultured in a humidified incubator with 5% CO2 at 37 ° C. After incubation for 48 hours, the medium was removed, and the flask was washed with culture medium. Then, 10 mL medium was added. The medium was changed every 72 hours.

When the confluency reached 80–90%, the cells were washed twice with 10 mL PBS, then removed from the flask by the adding 5mL 0.25% Trypsin/EDTA. It was then incubated for 5 minutes at 37 °C. After incubation, 10 mL culture media was added into the flask and mixed with pipetting. The suspension was transported into a 50 mL tube, centrifuged at 400xg for 5 minutes, aspirated and re-suspended with 10 mL fresh culture media.

Ten µL of cell suspension was diluted via 10 µL trypan blue to count the cells using a cell counter, and the total cell number was calculated. The cells were then transferred to new flasks at 1150 cells/cm^2 in fresh mesenchymal stem cell culture media, and incubated in a tissue culture incubator (at 37°C with 5% CO_2). These cells were preserved in the biobank for further studies. To assess the cell viability, the samples were stained with Trypan Blue (100 µL with 0.4% concentration for each sample), and examined using a sophisticated image analysis system with an auto-focus mechanism (The Countess II Automated Cell Counter, ThermoFisher, USA).

All cell culture and cell viability tests were conducted in triplicate, while RT-PCR experiments were performed in duplicate.

Mice Cell Line Culture and Cytotoxicity Test of NOHAL Solution

For the cytotoxicity test, the BALB/c 3T3 (CCL-163) cell line from ATCC was used. DMEM (Dulbecco's modified eagle medium) (ATCC Cat No: 30-2006) was used for cell culture, 10% (v/v) fetal bovine serum, antibiotics (penicillin/streptomycin; and 1% (2 mM) L-glutamine were added, and incubated in a humidified 5% CO_2 incubator at 37°C. A mixture of 0.25% trypsin and 0.03% EDTA was used for trypsinization, as suggested by ATCC. The cells were suspended in a culture medium and transferred to a 96-well plate, with 10^4 cells per well (100 µL).

Dose Administration Concentrations of Mice Cell Line Culture and Cytotoxicity Test of NOHAL Solution

After 24 hours of cell culture, the medium was removed and 100 µL of test material, positive control or negative control was added. All doses were applied with at least 5 repeats. After 48 hours, the plates were examined, and the culture medium was removed.

The culture medium was eliminated from the wells after examination of the plates. A 50 µL of MTT solution was added to each well. The plates were incubated at 37°C for 2 hours. Then, MTT solution was removed, and 100 µL of isopropanol was added to every well. Absorbance measurements were done using a microplate reader with a 570 nm filter, and then evaluated. A polyethylene tube was used as Negative Control (NC), DMSO (dimethyl sulfoxide) serial dilutions (30–10 v/v) were used as the positive controls (PC), and different concentrations of Test Material (TM) (100 −30-10 −3-v/v) were used.

The material was considered as cytotoxic if the survival rate of the test material was less than 70%. Survival value was determined according to the formula below:

Survival %= 100 x OD_{570TM} /$OD570_{NK}$

OD_{570TM} = The mean of the optical density value of the test material after blank is removed.

$OD570_{NK}$= The mean of the optical density value of the negative control after blank is removed.

SARS-Cov2 Infection of Human K18-hACE2-Transgenic Mice Models with Intranasal Delivery of NOHAL Solution

To test the effectiveness of NOHAL, an in vivo challenge experiment was designed. Three 8-to-10-week-old K18-hACE2 transgenic female (Jackson Lab, USA) mice were used in each group. The mice were randomly assigned to three groups: low-dose NOHAL1 solution [OZYS1000 ppm] group (Group I), high-dose NOHAL2 solution [OZYS1600 ppm] group (Group II), and placebo (PBS) group (Group III). A 50 µL of NOHAL1, NOHAL2 and PBS was delivered through intranasal (i.n.) instillation to the Groups I, II and III, respectively, for three days under anesthesia. After the application of the last intranasal spray, the animals were transferred to biocontainment IVC cages in the BSL 3 laboratory for the challenge experiment. Under anesthesia, the animals were infected intranasally with 50 µL of 10^5 $TCID_{50}$ SARS-CoV-2 virus, for three days. The nasal spray was administered in the morning, and the SARS-CoV-2 virus was given in the afternoon (Figure 1 – the schema of experimental design). The weights of all mice were measured daily.

Both applications were stopped when the challenge period was finished. The animals were observed until the 10th day of the experiment, and their daily weights were recorded. The animals were sacrificed with cervical dislocation, and gross pathologic examination was performed. For virus extraction, their lungs were harvested and an oropharyngeal lavage was done. Virus isolation was performed at −20°C.

Tissue Homogenization

The tissues harvested from each mouse were homogenized in 3 mL of PBS using an ultrasonic homogenizer at 70% amplitude, for 90 seconds (BANDELİN HD2200.2) for viral isolation. Tissue homogenates were centrifuged at 17,000x g for 10 minutes, and the supernatants were placed into 15 mL falcon tubes.

Viral RNA Isolation and qRT-PCR

QIAamp Viral RNA Mini kit Cat: 52906 (QIAGEN) was used in relation with the protocols to extract viral RNA. The viral RNA was quantified with One Step PrimeScript III RT-qPCR Kit (Takara). A CFX96 Touch instrument was used for all reactions under these quantitative-PCR conditions: 52°C for 5 min, 95°C for 10 sec, followed by 44 cycles at 95°C for 5 sec and 55°C for 30 sec. The CDS primer sequences used for RT-qPCR were targeted against the Nucleocapsid (NC) gene of SARS-CoV-2 with the following primers and probes: N1 Forward: 5′-GAC CCC AAA ATC AGC GAA AT-3′, N1 Reverse: 5′-TCT GGT TAC TGC CAG TTG AAT CTG-3′ N1 Probe: 5′-FAM-ACC CCG CAT TAC GTT TGG TGG ACC-BHQ1-3 N2 Forward: 5′-TTA CAA ACA TTG GCC GCA AA-3′ N2 Revers: 5′-GCG CGA CAT TCC GAA GAA-3′ N2 Probe: 5′-FAM-ACA ATT TGC CCC CAG CGC TTC AG-HQ1-3. RT-PCR experiments were performed in duplicate.

Irritation Studies of NOHAL Solution

Skin Irritation Test of NOHAL Solution

Information About the Irritation Test (TS EN ISO 10993-10:2010)

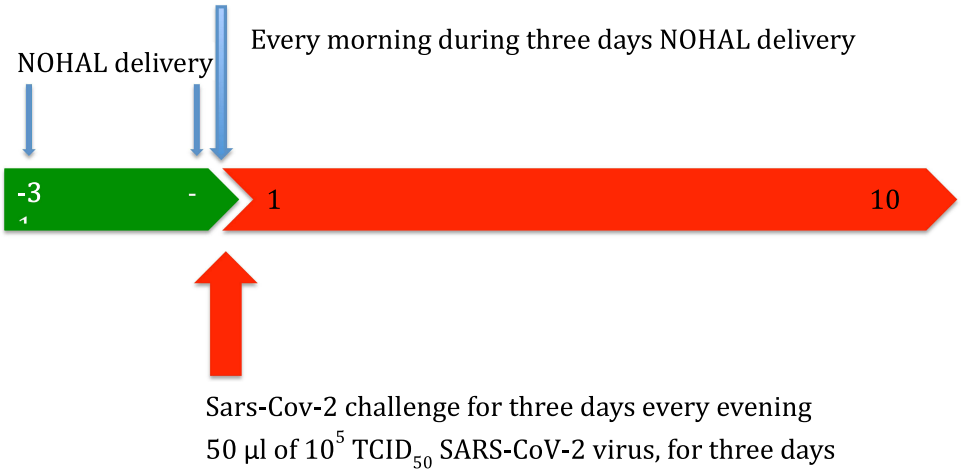

Figure 1 Schematic of experimental design.

The irritation test procedure was conducted in line with the following standards: Irritation test TS EN ISO 10993–10:2010, Animals and husbandry TS EN 15010993-2:2006, Preparing of the test material TS EN ISO 10993-12:2013.

The irritation test procedure was conducted in line with the following standards: Irritation test TS EN ISO 10993-10:2010, Animals and husbandry TS EN 15010993-2:2006, Preparing of the test material TS EN ISO 10993-12:2013.

Animal and Husbandry

As test animals, three healthy young New Zealand adult albino rabbits were used, weighing 2–3 kg. The areas to be treated were shaved and cleaned 24 hours before stimulation. Before the animals were taken into cages, the shaved areas were thoroughly washed with warm water and dried with a towel.

Preparation of the Test Material

The test material was applied according to the standards given under the title of TS EN ISO 10993-10: 2010 annex A A.2,2 Liquid test materials. According to the directive that liquids should be tested without dilution, the test material was given as l600 ppm.

Groups

The positive control was sodium lauryl sulfate (SLS), and the negative control was distilled water.

Application

NOHAL Solution product was kept in direct contact with the sample application areas no. 2 as shown in Figure 2. SLS impregnated gauze was applied to the positive control area (area 3). The samples were covered with gauze and fixed with a bandage, and contacted topically with the back skin for 4 hours.

Observation of Animals and Determination of the Irritation Index

The appearances of the application sites were recorded at (1 + 0.1) h, (24 + 2) h, (48 + 2) h and (72 + 2) h, after removal of the patches. To determine the irritation index, the skin reaction scoring system was used (Tables 2 and 3). The first hour, as specified in the standard, was not included in the calculation.

Oral Mucosal Irritation Tests of NOHAL Solution

Information About the Mucosal Irritation Test (TS EN ISO 10993-10)

The oral mucosal irritation test was carried out according to ISO 10993-10 standard. The laboratory animals were used in

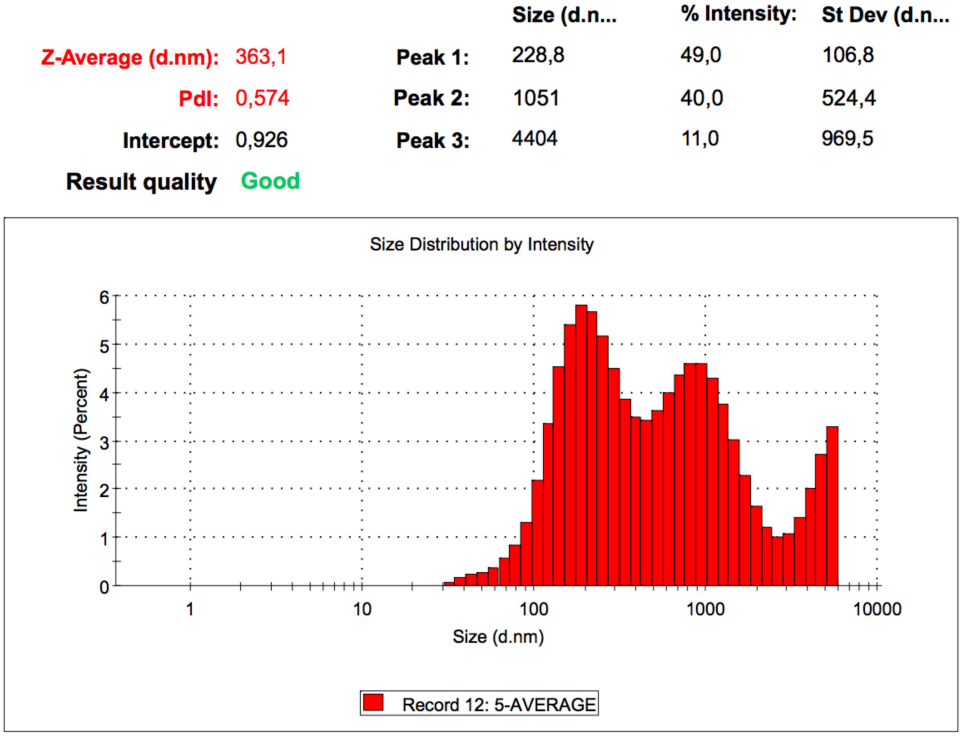

Figure 2 Zeta size and poly dispersity index of liposomes.

Table 2 Scoring System for Skin Reactions

Reaction	Irritation Score
Erythema and Eschar Formation	
No Erythema	0
Very Slight Erythema (barely perceptible)	1
Well-defined erythema	2
Moderate Erythema	3
Severe erythema (beet-redness) to eschar formation preventing grading of erythema	4
Edema formation	
No Edema	0
Very slight edema (barely perceptible)	1
Well-defined edema (edges of area well-defined by definite raising)	2
Moderate Edema (raised approx. 1 mm)	3
Severe edema (raised more than 1 mm and extending beyond exposure area)	4
Maximal possible score for irritation	8

the test in line with the ISO10993-2 standard, and the material was prepared in line with the 10993-12 standard. This test is performed for materials that are planned to come into contact with oral mucosa, and where safety data cannot be obtained by other means.

Test Animals and Care

The animals were familiarized with the environment as specified in TS EN ISO 10993-2: 2006. Healthy young adult Syrian hamsters of both sexes, unrelated from a single strain, were used for testing.

Groups

The material was tested according to the recommendation of ISO 10993-10 Annex A A.2.2 Liquid test materials: liquids should be tested without dilution or by direct precipitation, or diluted with a suitable liquid if not applicable. According to this directive, the test material was diluted with saline to 1/5 dose, which is the intended dose for its use. Gauze impregnated with the test material was placed in the left buccal sac, in direct contact with the mucosa of the buccal sac. The left inner buccal sac of each animal was used as the experimental sample, and the contralateral (right) inner buccal sac was considered as the control. No material was placed in the right inner buccal sac; it was used as a negative control and was dissected at the end of the experiment after washing with saline. As a positive control, based on the rule that liquids with pH 2 and below are considered irritants, HCl acid solution adjusted to a pH 1.5 was used.

Table 3 Evaluation Categories of Primary or Cumulative Irritation

Average Score	Response Category
0–0,4	Negligible
0,5–1,9	Mild
2–4,9	Moderate
5–8	Severe

Application

Under ketamine/xylazine anesthesia, the inner cheeks of Syrian hamsters were emptied and washed with physiological saline. Then, gauzes soaked with NOHAL solution were placed in the left buccal sac of each animal. The exposure time was evaluated according to the expected actual usage time of the material, and the experiment was carried out as 4 repetitions of 1 hour at intervals of half an hour. Considering the actual time of use, the gauze was kept in the buccal sac for 1 hour. At the end of each application, macroscopic observations were made and recorded.

Macroscopic and Microscopic Evaluation

Every macroscopic observation was recorded. The opposite cheek was washed with saline solution, ensuring that it was not contaminated. Experimental (left) and control (right) inner buccal sacs were macroscopically and microscopically examined, as outlined in Tables 4–6 (Scoring system for Oral reactions), respectively. According to the standard directive, the exposure time should reflect the actual time of use of the material, but should not be less than 5 minutes. Since it is a device with subacute use, the application was carried out for 1 hour in one go. The left inner cheek (device) observations were compared with the right inner cheeks, which were washed with saline (negative control).

After sacrifice, the buccal pouches were removed and prepared for histopathological examination. The sections were dewaxed, cleaned with xylene, and stained with conventional H & E method at room temperature.[52]

Hematoxylin–eosin (HE) stained sections were prepared from the inner cheek samples for histopathological

Table 4 Scoring System for Oral Reactions

Reaction	Irritation Score
Erythema and Eschar Formation	
No Erythema	0
Very Slight Erythema (barely perceptible)	1
Evident Erythema	2
Moderate Erythema	3
From severe erythema (beet-red) to eschar formation preventing grading of erythema	4
Other adverse changes in tissues should be recorded and reported.	

examination from the groups and were then examined under the microscope.

Nasal Irritation Test of NOHAL Solution

Animals were accustomed to the environment as specified in TS EN ISO 10993–2: 2006. Twelve (6 experimental animals and 6 controls) healthy, young, adult BalbC mice of both sexes, unrelated from a single strain, were used for testing. Four doses (4 x1 mL) of NOHAL were instilled into animals' nasal cavities over a period of 4 days.

In the experimental group, 1 mL of the solution, was dropped into the animals' nasal cavities once per day for 4 days. The same amount of saline was dropped into the animals' nasal cavities for 4 days in the control group.

Hematoxylin–eosin (HE) stained sections prepared from the nasal mucosa were examined under the microscope. Macroscopic and microscopic examination for the nasal mucosal irritation test was made by considering the parameters outlined in Tables 4 and 6, respectively.

Table 5 Irritation Index

Irritation Index	
0	None
1–4	Least
5–8	Mild
9–11	Medium
12–16	Severe

Table 6 Grading System for Microscopic Examinations of Oral and Nasal Tissue Reactions

Reaction	Score
Epithelia	
Normal, sturdy	0
Cell Degeneration or Flattening	1
Metaplasia	2
Focal Erosion	3
General Erosion	4
Leukocyte infiltration (for high penetration areas)	
None	0
Least (less than 25)	1
Mild (26 to 50)	2
Medium (51 to 100)	3
Prominent (greater than 100)	4
Vascular congestion	
None	0
Least	1
Mild	2
Medium	3
Prominent, along with destruction of the veins	4
Edema	
None	0
Least	1
Mild	2
Medium	3
Prominent	4

Ocular Irritation Test of NOHAL Solution

Animals and Husbandry

Three healthy young adult albino rabbits of both sexes, from a single strain, weighing 2 kg to 3 kg, were used for the test. The animals were housed under ambient conditions, as specified in ISO 10993-2.

Application

Up to 24 hours before the start of the experiment, both eyes of each rabbit were visually examined to identify any ocular abnormalities. Two percent sodium fluorescein BP

(British Pharmacopoeia) can be used to visually detect any corneal damage. A normal cornea is not stained by fluorescein; however, conjunctival abrasions are seen as yellow or orange, corneal abrasions or ulcers are seen as bright green, and foreign bodies are observed to be surrounded by a green ring after application of fluorescein.

A 0.1 mL test solution was applied to the lower conjunctival sac of one eye, without any dilution. After placing the test material in the conjunctival sac, the eyelids were kept closed for approximately 1 hour. Fluorescein-treated eyes were then examined macroscopically and with a slit-lamp microscope by an ophthalmologist to ensure that the cornea was undamaged.

Observation of Animals and Determination of the Irritation Index

The animals were examined at 1 (± 0.1) h, 24 (±2) h, 48 (±2) h and 72 (±2) h. Since no lesions were observed, the observations did not need to be extended for longer periods.

Observations were graded according to the grading scale for ocular lesions, as presented in Table 7.

Results

Liposome Characterization

NOHAL solution dimensions ranged between 30 nanometers and 5 microns. The majority of the particles were found to be concentrated at 228.8, 1051 and 4404 nanometers (Figure 2). The polydispersity index (PDI) was 0.574 for NOHAL. Zeta potential value was neutral (−3mV). The conductivity was 15.7mS/cm. The pH of the solution was measured as 4.02 with a Mettler-Toledo MP220 pH meter.

Analysis of Time-Dependent Antibacterial Effects of NOHAL Solution

After determining the MIC, *Staphylococcus aureus* (ATCC 6538), *Streptococcus pneumoniae* (ATCC 49619) and *Escherichia coli* (ATCC 25922) suspensions (2000, 1750, 1500, 1250 ppm) were added to the solutions, 0.5 McFarland turbidity was adjusted, and prepared above and below the determined MIC value. The final concentrations of the solutions were set to initial levels of 2000, 1750, 1500, 1250 ppm. The samples were collected at 2 min, 10 min, 30 min, 1 h, 2 h, 3 h, 4 h, 5 h, and finally, 6 h from the solutions. Blood agar medium (Germany-Becton Dickinson) was used to cultivate the collected samples, which was incubated at 37 °C. *Streptococcus pneumoniae* (ATCC 49619), which is a temporary flora element in the upper airways and the primary agent of community acquired pneumonia, was added to our study and evaluated in terms of antibacterial efficacy of NOHAL. Any bacterial growth was inspected in the plates after being incubated for 24 h. The inhibition values were recorded for the plates without any growth of bacteria (Table 8).

Stability Test of NOHAL Solution

ASTM F1980 (standard guide for accelerated aging of sterile barrier systems for medical devices) was taken as the reference to prepare the ozone solutions in their active concentrations, and the solutions were stored at 55 °C for 37 days to determine their stability after one year. After one year, *Staphylococcus aureus* (ATCC 6538) and *Escherichia coli* (ATCC 25922) suspensions regulated to 0.5 McFarland turbidity were added to the solutions again. As before, the samples were obtained from the solutions at 2 min, 10 min, 30 min, 1 h, 2 h, 3 h, 4 h, 5 h, and finally, 6 h (Table 9). Blood agar medium (Germany-Becton Dickinson) was used for cultivation of the samples and they were incubated for 24 h at 37 °C. The presence of bacterial growth was assessed on the plates after the incubation period. The stability was defined as preserved effectiveness of the solution during the contact period, at the concentration where the antibacterial activity was previously recorded.

In vitro Anti-Viral Activity

The results of the in vitro study demonstrated that NOHAL solution decreased the viral load, as a predictor of anti-viral activity for COVID-19, in a time- and concentration-dependent manner. There were significant decreases between the input and final concentrations after NOHAL treatment in the samples that underwent 1600 ppm exposure for 30 seconds and 5 minute incubation time, and also 1000 ppm exposure for 5 minutes incubation time. As shown in Figure 3A, the most significant effective values for the solution were 1000 ppm for 5 minutes, and 1600 ppm for 30 seconds, and 1 and 5 minutes. 1600 ppm showed greater in vitro antiviral effect compared to 1000 ppm. Moreover, Figure 3B exhibits the final cDNA concentration when the solution was added into the cell culture.

Table 7 Observations Were Graded According to the Grading Scale of the Ocular Lesions

Reaction	Numeral Rating
1- Cornea	
Degree of opacity (at peak area)	
No opacity	0
Scattered or spread areas, details of the iris clearly visible	1*
Easily distinguishable translucent areas, details of iris slightly blurred	2*
Opaque areas, details of the iris are not visible, pupil size is difficult to distinguish	3*
Opaque, iris details cannot be seen	4*
Corneal area affected	
One quarter (or less), not zero	0
Larger than a quarter, less than half	1
Larger than half, but less than three-quarters	2
Larger than three-quarters, to the entire area	3
2-Iris	
Normal	0
Abnormal curl, congestion swelling, corneal injection (either or all or a combination of these), iris still responding to light (lazy reaction positive)	1*
Unresponsive to light, bleeding, major destruction (any or all)	2*
3. Conjunctivae	
Redness [palpebral and bulbar conjunctiva with exception of cornea and iris]	
Normal blood vessels	0
Blood vessels are filled, above normal	1*
More common, deep crimson red, each blood vessel is not easily distinguishable	2*
Widespread beefy red	3*
Chemosis	
No swelling	0
Abnormal swelling (including nictitating membrane)	1*
Significant swelling with partial outward rotation of eyelids	2*
Swollen with semi-closed eyelids	3*
Swollen with approximately half closed to fully closed eyelid	4*
Discharge	
No discharge	0
Any amount other than normal (except small amounts observed in normal animals)	1
Discharge with moistening of eyelids and adjacent hairs	2
Moistening of eyelids and hairs in a significant area around eyes	2

Note: *Positive result.

Table 8 Tests of *Staphylococcus aureus* (ATCC 6538), *Escherichia coli* (ATCC 25922), *Streptococcus pneumoniae* (ATCC 49619) at Different Ppm Levels and Different Durations

A. *Staphylococcus aureus*				
NOHAL Solution			***Staphylococcus aureus* (ATCC 6538)**	
Time	**2000 ppm**	**1750 ppm**	**1500 ppm**	**1250 ppm**
2 min	+	+	+	+
10 min	+	+	+	+
30 min	+	+	+	+
1 h	Reduction	+	+	+
2 h	–	–	–	Reduction
3 h	–	–	–	_
4 h	–	–	–	–
5 h	–	–	–	–
6 h	–	–	–	–
B. *Escherichia coli*				
NOHAL Solution			***Escherichia coli* (ATCC 25922)**	
Time	**2000 ppm**	**1750 ppm**	**1500 ppm**	**1250 ppm**
2 min	+	+	+	+
10 min	+	+	+	+
30 min	Reduction	Reduction	+	+
1 h	–	–	–	–
2 h	–	–	–	–
3 h	–	–	–	_
4 h	–	–	–	–
5 h	–	–	–	–
6 h	–	–	–	–
C. *Streptococcus pneumoniae*				
NOHAL Solution			***Streptococcus pneumoniae* (ATCC 49619)**	
Time	**2000 ppm**	**1750 ppm**	**1500 ppm**	**1250 ppm**
2 min	+	+	+	+
10 min	+	+	+	+
30 min	Reduction	+	+	+
1 h	–	–	Reduction	Reduction
2 h	–	–	–	4 colonies
3 h	–	–	–	_
4 h	–	–	–	–
5 h	–	–	–	–
6 h	–	–	–	–

Table 9 ASTM F 1980 Stored at 55°C for 37 Days NOHAL Solution

Time	*Staphylococcus aureus* (ATCC6538)	*Escherichia coli* (ATCC25922)
2 min	Present	Present
10 min	Present	1 colony
30.min	Present	1 colony
1 hour	20 colonies	Absent
2 hour	Absent	Absent
3 hour	Absent	Absent
4 hour	Absent	Absent
5 hour	Absent	Absent
6 hour	Absent	Absent

In vitro Cell Viability Tests of NOHAL Solution

The cell viability rates are shown in Figure 4A, which indicates that this solution did not affect cell viability in a toxic manner. Most interestingly, the in vitro cell viability effect of the 1600 ppm NOHAL solution on transfected cells tended to be higher when compared to other concentrations and incubation periods. However, the noted superior effect of 1600 ppm with longer incubation times was not statistically significant. This was particularly obvious at 24 hours, even at the highest solution concentration used in the study when the antiviral activity rate was the highest (Figure 4A). The flow cytometry result of 7AAD marker for viability of human primary lung epithelial cells is shown in Figure 4B.

Rotary Cell Culture System 3-D Cell Culture Studies

The actual effect of this solution was studied by mimicking the in vivo conditions via a 3-D RCCS, comprised of three basic steps; bioreactor loading, vessel rotating, and addition of the treatment scheme. In our study, we used 3D modeling by the primary cell culture by including multiple cell types, containing pulmonary fibroblasts and epithelial airway cells. 3-D systems also mimic the cell-to-cell interactions and their tissue microenvironment by affecting the cell types surrounding them, intercellular adhesions, and by creating growth factor and cytokine gradients. On the other hand, 2D cell cultures lack the hierarchy and dynamic complexity of even the plainest in vivo investigations. The results of the treatment with NOHAL solution clearly showed that there was no inter-donor variations or toxic effects. On the other hand, it increased the survival time of the cells up to 16 days, compared to the normal time of 11–14 days. It also increased the cell proliferation rate without any effect on the cell viability (Figure 4C). Periodic cell viability assessment via Trypan Blue staining was performed as an early indicator of the quality of the cells, and during the studies, all cell viabilities were greater than or equal to 96% in both the untreated and treated groups.

Mesenchymal Stem Cells Studies

Cell viability assays were performed using Trypan Blue dye, and examined using image analysis system (The Countess II Automated Cell Counter, ThermoFisher, USA). All cell viabilities were greater than or equal to 96% confluency (Figure 5A). There was no negative effect of NOHAL solution on mesenchymal stem cells (Figure 5B); on the contrary, NOHAL solution affected the cell viability positively (Figure 5C).

Results of Cytotoxic Effects

If the survival rate of the test material is less than 70%, the material is considered as cytotoxic.

According to the results of the test conducted in accordance with the directives of the TS EN ISO 10993–5 standard, the NOHAL solution did not show any cytotoxic effects when compared with the control group (Table 10, Figure 6A and B). However, cytotoxic effects were seen on cell viability in the positive control (Figure 6C).

The SARS-CoV-2 qRT-PCR Virus Loads of the Lung Samples and Oropharyngeal/ Nasal Wash Fluids

Lung samples and oropharyngeal/nasal wash fluids were collected from each animal on day 10, and their viral loads were measured using qRT-PCR. Significantly lower Cycle Threshold (CT) values were detected in mice treated with PBS (Figure 7) and NOHAL1 Solution compared to NOHAL2 treated mice (Figure 8). The CT values of three experimental groups are presented in Table 11.

The effect of the solution was better at 1600 ppm. The viral load in the lung with "a very high CT value" was found to be insignificantly low. No virus was found in the nasal or oropharyngeal wash fluids, there was no

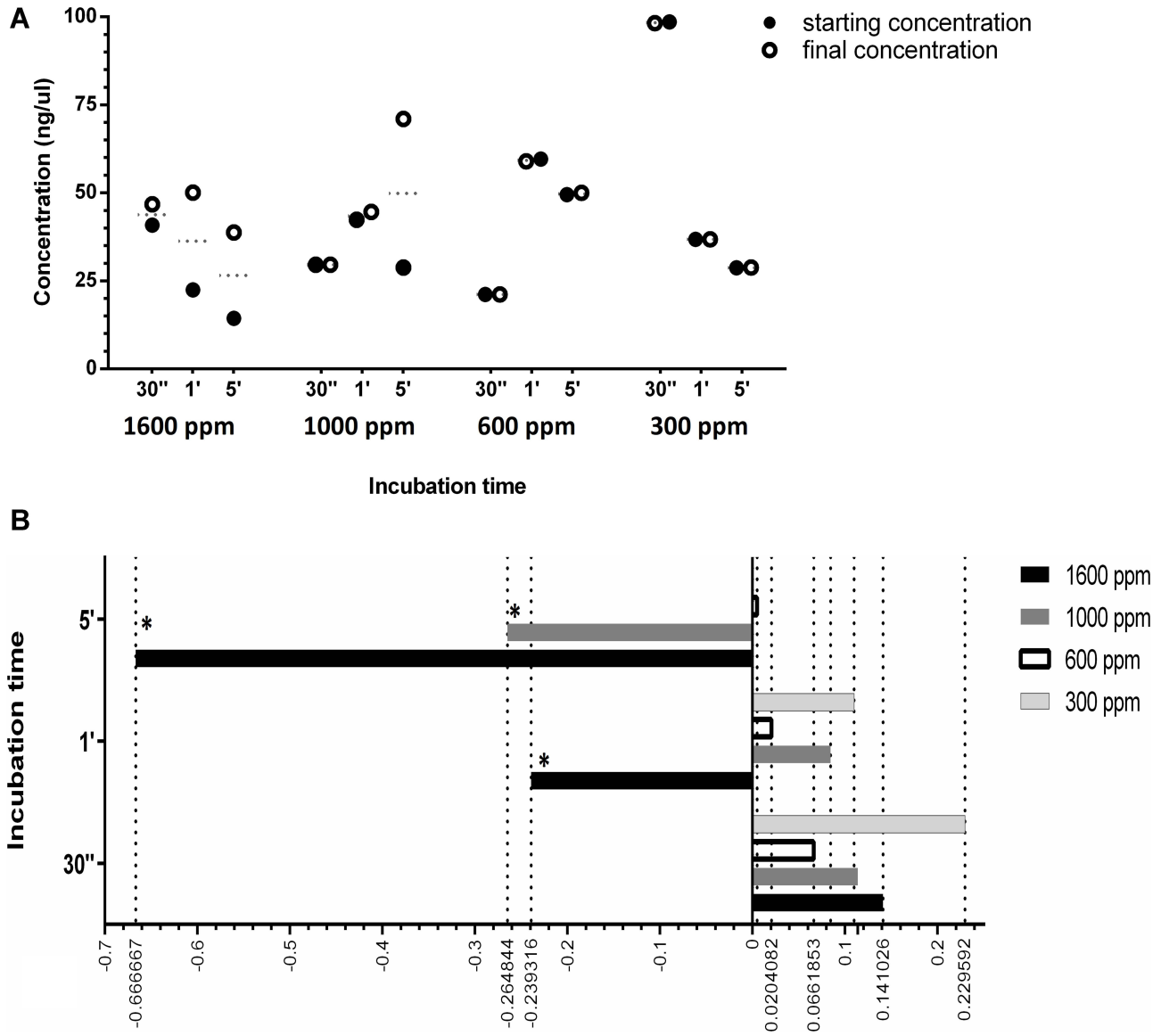

Figure 3 (**A**) Antiviral activity in time with different concentrations of NOHAL solution. (**B**) Fold change of the final cDNA concentration with different concentrations of HA NOHAL solution. Statistical comparison were made using median values of duplicates. Groups with significant changes were indicated using asterisks.

reading on qRT-PCR, and it was evaluated as zero. Even when the nasal spray was applied once a day, the viral load in both nasal oropharyngeal wash fluids and lung was found to be zero in mice that had a dose of 1600 ppm, and this dose prevented pneumonia formation in the lungs.

Body Weight

The mean weight in each cohort was similar to the pre-infection weights. In the experimental groups, all mice lost weight. According to the 10th day measurements, it was determined that they gained weight, and all successfully finished the experiment. The weights were recorded daily.

Macroscopic Examination of the Lungs

Gross pathologic examination of the PBS-treated group showed multifocal consolidations with a patchy distribution pattern. Parenchymal and subpleural petechiae and hemorrhage were prominent in some of the animals (Figure 9A). All animals' lungs were edematous, and

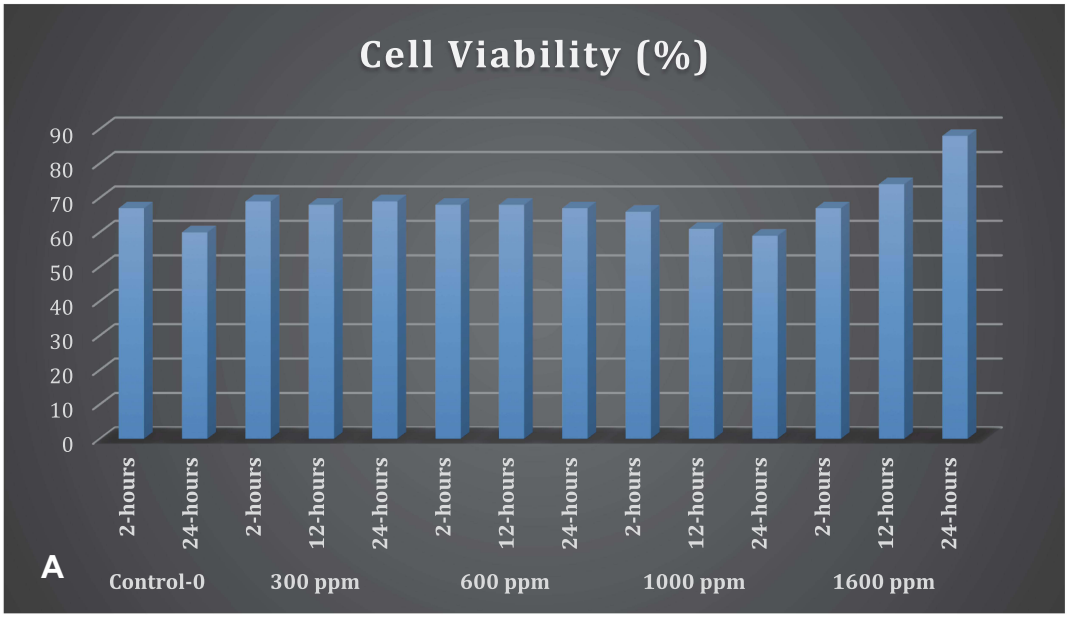

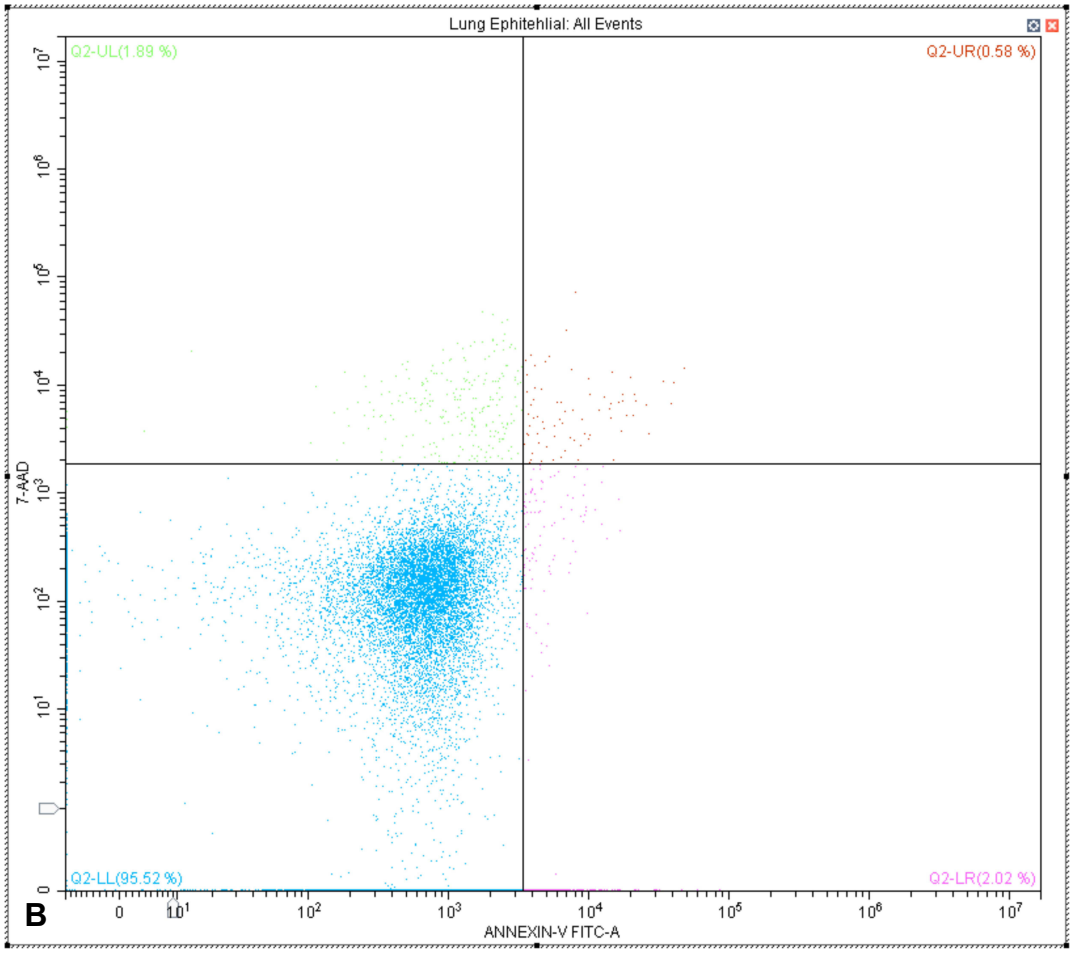

Figure 4 Continue.

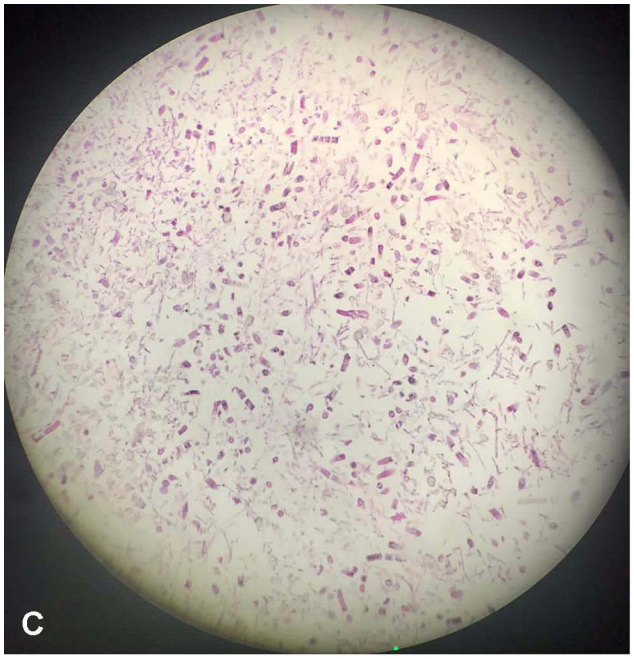

Figure 4 (**A**) Concentration- and time-dependent cell viability ratio changes with NOHAL treatment. (**B**) Flow cytometry image of 7AAD marker for viability of human primary lung epithelial cells. (**C**) Primary 3D cell culture of pulmonary fibroblasts and airway epithelial cells: no toxic effect is present (H&E staining).

their mean lung weights were elevated. The lungs of the nasal NOHAL applied animals showed no significant changes, and their lung parenchymas were pink and homogeneous (Figure 9B and C).

These results indicated that 1600 ppm solution was protective against SARS-CoV-2 infection in the nasal/oropharyngeal regions and the lungs.

Results of Irritation Tests

Results of Skin Irritation Test (TS EN ISO 10993-10:2010)

For the test material, the mean score was calculated according to the observation values made in three different time periods (24. 48. 72. h). In the observations, no erythema or edema was observed during the application of test samples. In the positive control, erythema and edema was observed (Figure 10) (Tables 12 and 13).

According to the results, it was found that the test specimen "NOHAL Solution" did not have any irritating properties specified in TS EN ISO 10993–10:2010.

Results of the Oral Mucosal Irritation Test (TS EN ISO 10993-10:2010)

Macroscopic observations and analyses were made in relation with TS EN ISO 10993-10: 2010 standard. On macroscopic examination (Table 14), no irritation (erythema or ulcers) (Figure 11A) was observed in inner cheek pouch mucosa, similar to controls (11c). Mucosal erosion areas were noted in the positive controls (Figure 11B). The mean irritation index was calculated as zero (0) for each animal, except for the positive controls.

When the hematoxylin–eosin (HE) stained tissues prepared from the inner buccal samples of the test product group were examined under the microscope, no erosion or ulceration, leukocyte infiltration or vascular congestion were found in the mucosa or the epithelium (Figure 12A and B). The mean irritation index was calculated as zero (0) for each animal in the experimental group. In positive controls (Figure 12C), the index averaged 6, while it was calculated to be a maximum of 8 and a minimum of 5 and determined as moderate. Oral microscopic irritation scores are given in (Table 15).

Results of the Nasal Mucosal Irritation Test (TS EN ISO 10993-10:2010)

The results of the microscopic examinations made in accordance with TS EN ISO 10993–10: 2010 standard are presented in Tables 4 and 6. Under macroscopic examination, there was no evidence of irritation (erythema or ulcers) in the nasal mucosa, similar to the controls. The mean irritation index was calculated as zero (0) for each animal in the experimental group (Table 16). Hematoxylin–eosin (HE) stained nasal samples were examined under the microscope for erosion or ulceration in the epithelium, leukocyte infiltration, and vascular congestion. According to the light microscopy, there was no evidence indicating any irritating effect of the of the NOHAL solution in the nasal mucosal samples of the animals (Figure 13). The results of the macroscopic and histopathological examination of the nasal mucosa showed that the NOHAL solution did not have any irritant effects on the nasal mucosa.

Results of the Ocular Irritation Test (TS EN ISO 10993-10:2010)

Both eyes of the animals were examined approximately 1 (± 0.1) hour after applying 0.1 mL of NOHAL solution to the left eyes of the animals. There was no sign of conjunctival irritation due to the application. Since there was no permanent damage or other signs of corneal irritation on the examination performed using 2% sodium fluorescein drops, there was no need to extend the observation period. The examination findings were graded according to the criteria presented in Table 17. Two percent sodium fluorescein does not stain normal cornea. There was no fluorescein staining in NOHAL treated left eyes of the

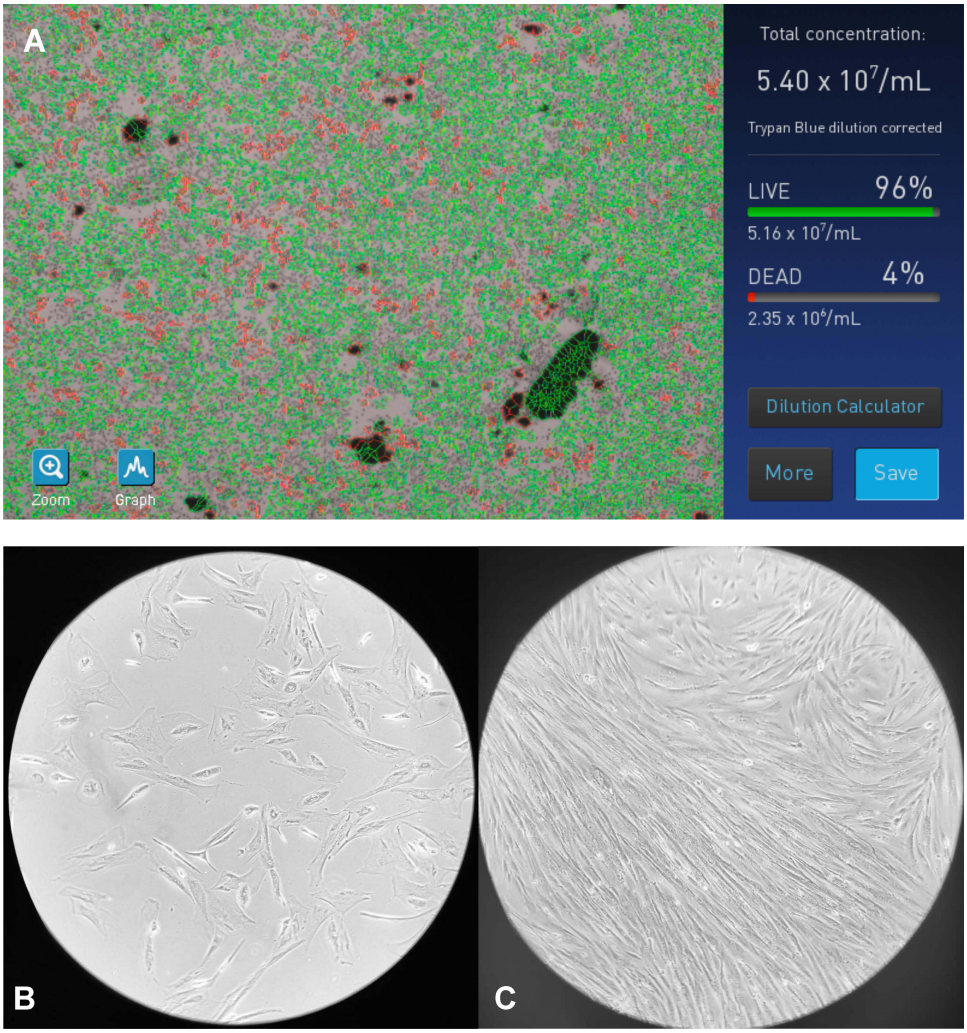

Figure 5 Cell culture studies. (**A**) 96% confluency is present. (**B**) Mesenchymal stem cells: no negative effect on cell viability. (**C**) Mesenchymal stem cells: positive effect of different concentrations on cell proliferation.

rabbit, and therefore, no positive reactions were observed in any animal. There were no ocular findings in the animals including peeling of the conjunctival membrane or mild ulceration, corneal perforation, blood or pus in the anterior chamber of the eye, bloody or purulent discharge, or severe corneal ulceration.

Table 10 Results of Quantitative Measurements of Cytotoxic Effects with MTT Test

Analysis Result								
	Mean of Optical Density (OD) at 570 nm ± Standard Deviation (SD)				**Survival %**			
	% Dilution Concentrations (v/v)				**% Dilution Concentrations (v/v)**			
	100	30	10	3	100	30	10	3
Test Material	0.244±0.08	0.276±0.05	0.29±0.03	0.31±0.06	76.25	86.25	90.62	96.87
Negative Control	0.32±0.05				100			
Positive Control		0.078±0.02	0.1±0.06			24.37	31.25	
BLANK	0.046±0.002							

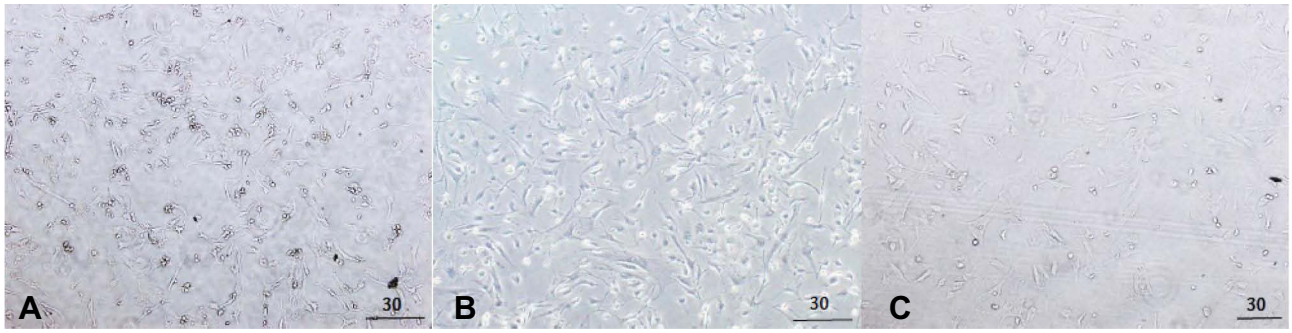

Figure 6 Photomicrographs of BALB/c 3T3 (CCL-163) cell line cultures. (**A**) NOHAL solution, (**B**) negative control, (**C**) positive control dimethyl sulfoxide (DMSO).

Figure 7 Representative photos from all groups showing (**A**). PBS control (PBS) group, pneumonia formation is observed in both lobes starting in the periphery and progressing towards the median. (**B**) NOHAL 1000ppm dose: no infection was observed in mouse lung in gross pathology. (**C**) NOHAL 1600ppm dose: no infection was observed in the mouse lung in gross pathology.

When the control (Figure 14A) and the tested eyes were compared in the ocular irritation experiment of the NOHAL solution, it was determined that there was no difference, and the NOHAL Solution material did not cause any changes indicating irritation of the ocular structures (Figure 14B and C) (conjunctiva, cornea or iris).

The results of the "Ocular Irritation Test" made in accordance with the directives of the TS EN ISO 10993-10: 2010 standard showed that NOHAL did not have any irritant effects in the eye.

Discussion

In 2019, a new severe acute respiratory syndrome coronavirus (SARS-CoV-2) was discovered in of the city of Wuhan, China. SARS-CoV-2 has caused one of the biggest pandemics in global history, causing more than 5,258,028 deaths thus far, as reported by WHO (12.04.2021).

In hospitals, dental offices and public places, SARS-CoV-2 both is highly prevalent in both saliva droplets and as aerosols, which means that COVID-19 transmission is not traceable to an index case, since the particles remain airborne for a period of time, then largely land across horizontal surfaces. Yoon et al indicated that SARS-CoV-2 was present in nasopharyngeal secretions, while oral secretions had a high viral load, particularly in the early phase of the infection and it was detected in the oral fluids of 91.7% of patients with COVID-19.[53] As we know, oral fluid is a significant factor in infection transmission; infected individuals produce saliva droplets containing microorganisms by coughing and sneezing. For this reason, it is possible that SARS-CoV-2-loaded droplets may infect the host via the mouth, nose or eyes, or may directly be inhaled into the respiratory tract.

Zou et al reported that nasal swabs showed higher viral loads than throat swabs in symptomatic patients. The same pattern was observed in asymptomatic cases,[54] showing that the nasal epithelium is one of the main portals for initial infection and transmission. The oral cavity is another portal for the initiation of the infection, and plays a role in the transmission of SARS-CoV-2.

Entrance of the coronaviruses into the cells depends on the affinity of the spike (S) protein to bind a specific receptor on the cell (hACE2), and consequent cellular protease-related priming of the S protein. This binding has also been indicated as a significant factor for SARS-CoV replication as well as progression of the disease.[55,56]

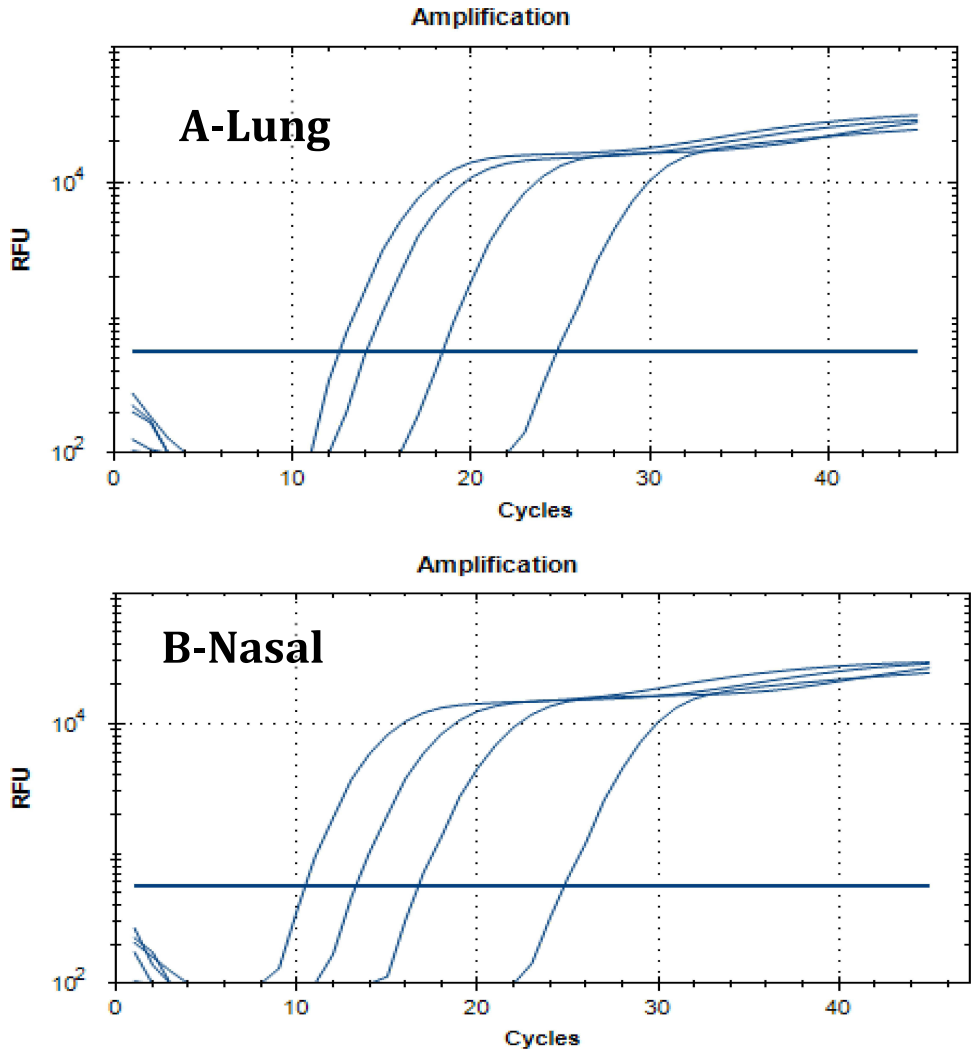

Figure 8 Representative CT values of PBS group in RT-PCR (**A** and **B**).

Entrance of the virus also depends on protease TMPRSS2, and the activity of one of its possible substitutes, cathepsin B/L.[57–59]

More recently, it has been shown that the hACE2 receptor, used by SARS-CoV-2 to establish infection, is highly expressed in the nasal epithelium,[60] oral epithelium[61] and cornea.[62] Since both nasal and oral epithelia are important reservoirs of SARS-CoV-2, the hygiene of these cavities could be important in the battle for COVID-19 pandemic.

The most common methods used to defend these routes include the use of personal protective equipment, careful hygiene, and distancing of individuals. However, despite all these physical protection barriers, transmission is still possible. Therefore, it is extremely important to reduce the viral load in the body regions responsible for transmission.[63,64]

It has been widely accepted that the application of nasal antimicrobial solutions reduces nasal viral load. Keeping the nasal cavity clean, maintaining a healthy mucosa and patent nasal passages prevents the virus from attaching to the nasal epithelial cells.[65,66]

Ludwig et al showed that mechanical nasal irrigation reduces the viral load.[67] The use of hypotonic solutions has also been shown to soften the mucus, and remove other pathogens such as bacteria and viruses adhering to the mucosa.[68] Over the previous year, new solutions have been tried for mouth and nasal mucous membranes in order to combat the COVID-19 pandemic. At the same time, many studies have investigated the effectiveness of previously used antibacterial products on SARS-CoV-2. Several oral and nasal antiseptics such as saline solutions,[66] Iota-carrageenan,[67] hypochlorous acid,[68] low pH Hypromellose,[69] PVPI,[70,71] cyclodextrin[72,73] and

Table 11 The NC1 and NC2 Regions of the SARS-COV2 Virus Were Examined Together with Viral RNA

Solutions	Animal Number	Lung	Nasal Wash
PBS	1	18/20	21/23
	2	12/11	15/15
	3	14/15	16/17
NOHAL1 1000ppm	1	20/20	24/24
	2	31/32	31/32
	3	34/35	36/36
NOHAL2 1600ppm	1	36/35	0/0
	2	36/35	0/0
	3	37/36	0/0

Notes: In the PBS group, a disease occurred right after infection, and CT was given early because the samples contained a high viral load. The positive control qPCR yielded CT at 23 for this study. PBS group animals yielded low numbers of CT. Accordingly, CT values up to 10–28 and 28–30 are considered positive, with the high viral load available. Late CT values between 35–40 are considered insignificant due to the very low viral load available (between 100–1000 copies). Since the device cannot read in the absence of viral load, these samples are evaluated as 0 (zero).

chlorhexidine[74] have been used to reduce viral load. In some studies, ozone has also been studied for nasal irrigation[75] and rectal insufflation.[23]

Several studies investigated the possible antiviral activity and therapeutic applicability of systemic ozone treatment in COVID-19 patients. Ozone therapy is thought to have an immunological effect among the possible treatments for SARS-CoV-2 pneumonia, since it plays a role in the modulation of cytokines and interferons. Therefore, there is an increasing interest in ozone therapeutics in the prevention and treatment of COVID-19.[76,77] More recently, a study used a molecular modeling approach and investigated the reactivity of ozone on the key molecules of SARS-CoV-2, where the results indicated that ozone could be an effective oxidant against SARS-CoV-2. It was also reported that it had the capability to attack the viral spike and envelope proteins and lipids, and may damage viral integrity.[78]

The powerful antibacterial and antiviral effects of ozone are well known. Gaseous ozone is widely used for environmental disinfection and in the medical field. However, due to the fact that ozone is not a stable gas, it has a limited area of use. At the same time, the fact that ozone applications can only be performed with ozone generators prevents its widespread use. However, in the present study, we encapsulated an O_3 molecule in a liposome with HA and glycerin in the liquid form. HA, which has water-retaining properties with nanoscale liposomes, provides both healing effects and moisturizes the mucosa.[79,80] At the same time, HA liposomal gels carry a strong potential for drug delivery, as has previously been demonstrated in in vivo applications.[81] Since the MW of HA causes different activities, choosing the HA size is a crucial factor. Various authors have studied all MW of HA, from high to low MW.[82] In this study, we decided to restore liposomes with 30–150 kDA MW of HA. As mentioned above, liposome dimensions ranged between 200 nm and 250 nm, and the HA-liposomes' particle size increased as the MW increased, as reported previously.[82] We were able to restore liposome surfaces efficiently with that MW HA (mean particle size increased in correlation to MW of HA), with a good polydispersity index (<0.7).[83] HA and glycerin make a good pair with tissue-improving effects in the cosmetic sector. Glycerin is also used to build stable lipid nanoemulsions.[1,84]

The preventive effect of ozone is at the forefront, and it differs in content from other oral and nasal rinsing products, owing to its HA decorated nanoliposome structure.

In our study, it has been proven by multiple experiments, including in vitro cell culture and in vivo transgenic mouse experiments, that the designed NOHAL solution has a strong antiviral effect on SARS-CoV-2. In addition, it has antimicrobial effects, while all biocompatibility and toxicity tests (skin, oral, nasal, eye) of the product have been performed, and in all experiments, no toxicity was reported. In terms of future directions in this study, more animals should be tested and clinical studies[71,73] should be encouraged for NOHAL solution as a translational medicine product.

Although there are still no medicines there are now effective vaccines[85] for COVID-19. However, personal protective equipment is still needed since all populations cannot be vaccinated at the same time, and the success rate of vaccination varies in different populations. For this reason, the only available alternatives to slow down the viral transmission are the local infection control procedures.

Conclusion

In this study, HA-decorated ozonated nanoliposome formulation inactivated SARS-CoV-2 efficiently in both dose- and time-dependent manners. Therefore, ozone has the potential to be used as a protective disinfectant for SARS-CoV-2. Most importantly, the product

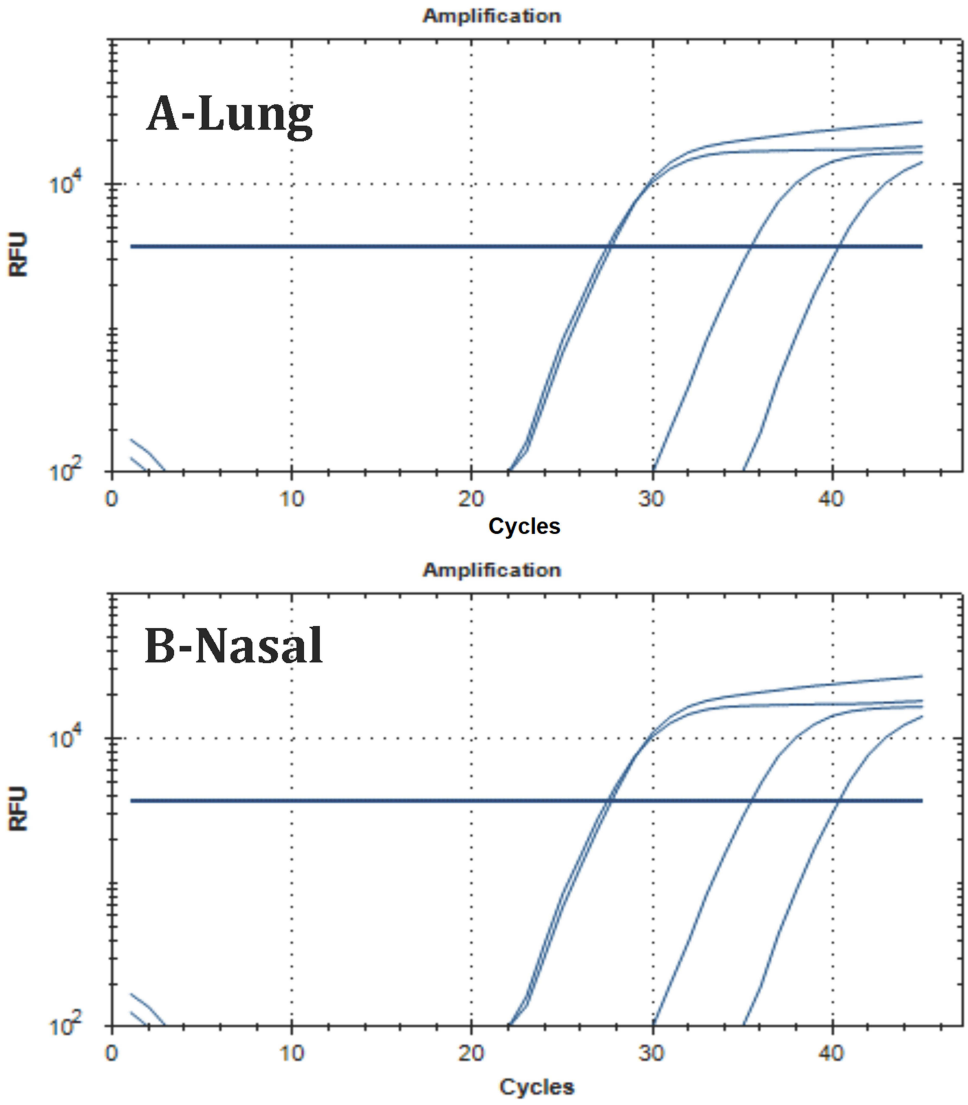

Figure 9 Representative CT values of NOHAL group in RT-PCR (**A** and **B**).

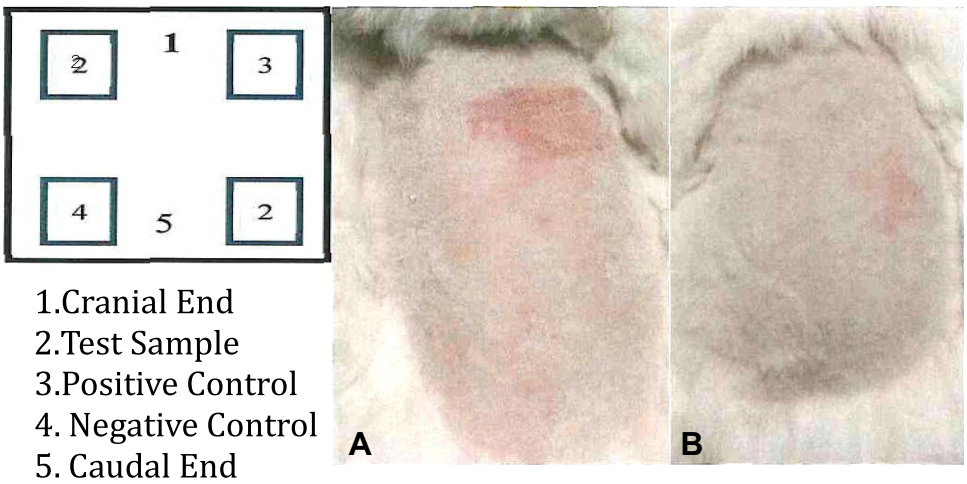

Figure 10 Application sites and irritation appearance at 24 (**A**), 48 (**B**) hours: it is observed that there is no irritation effect according to the positive control.

Table 12 Skin Irritation Test Scores

Animal Number	Groups	Application Sites	Observation							
			Erythema				Edema			
			1 Hour	24 Hour	48 Hour	72 Hour	1 Hour	24 Hour	48 Hour	72 Hour
1	**Sample**	Left Front		0	0	0	0	0	0	0
		Right Back		0	0	0	0	0	0	0
	Positive Control	Right Front	4	4	3	1	3	2	2	1
	Negative Control	Lelt Back	0	0	0	0	0	0	0	0
2	**Sample**	Left Front	1	1	0	0	0	0	0	0
		Right Back	0	0	0	0	0	0	0	0
	Positive Control	Right Front	3	3	2	1	3	2	0	0
	Negative Control	Lelt Back	0	0	0	0	0	0	0	0
3	**Sample**	Left Front	0	0	0	0	0	0	0	0
		Right Back	0	0	0	0	0	0	0	0
	Positive Control	Right Front	3	3	2	1	2	2	1	0
	Negative Control	Lelt Back	0	0	0	0	0	0	0	0

Table 13 Average of Skin Irritation Scores

Samples	Primary Irritation Score			Primary Irritation Index
	Rabbit 1	Rabbit 2	Rabbit 3	
Sample +SD	0.0 ±0.0	0.083 ±0.289	0.0 ±0.0	0.027
Positive Control +sD	2.167±1.169	1.333±1.211	1.500±1.049	1.666
Negative Control +SD	0.0±0.0	0.0±0.0	0.0±0.0	0.0

Table 14 Oral Macroscopic Irritation Score

Animal Number	Application Areas	Observation	
		Erythema	Eschar
1	Left Cheek (Test)	0	0
	Right Cheek (Negative Control)	0	0
2	Left Cheek (Test)	0	0
	Right Cheek (Negative Control)	0	0
3	Left Cheek (Test)	0	0
	Right Cheek (Negative Control)	0	0
Positive Control	Left Cheek (Test)	3	2

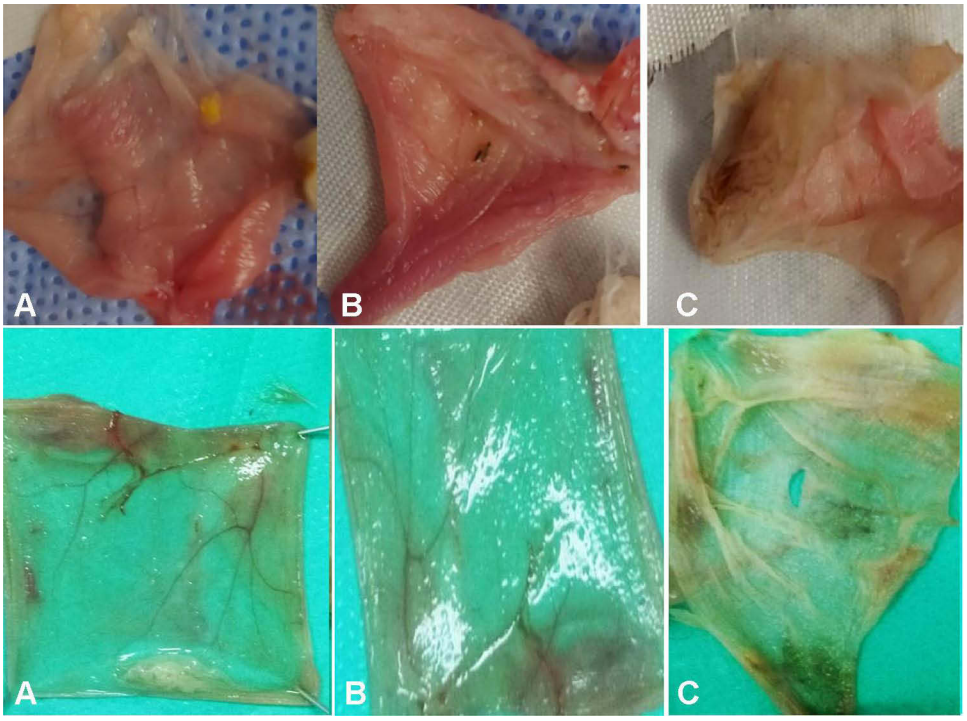

Figure 11 Macroscopic view of inner cheeks, (**A**) NOHAL (**B**) negative control (**C**) positive control.

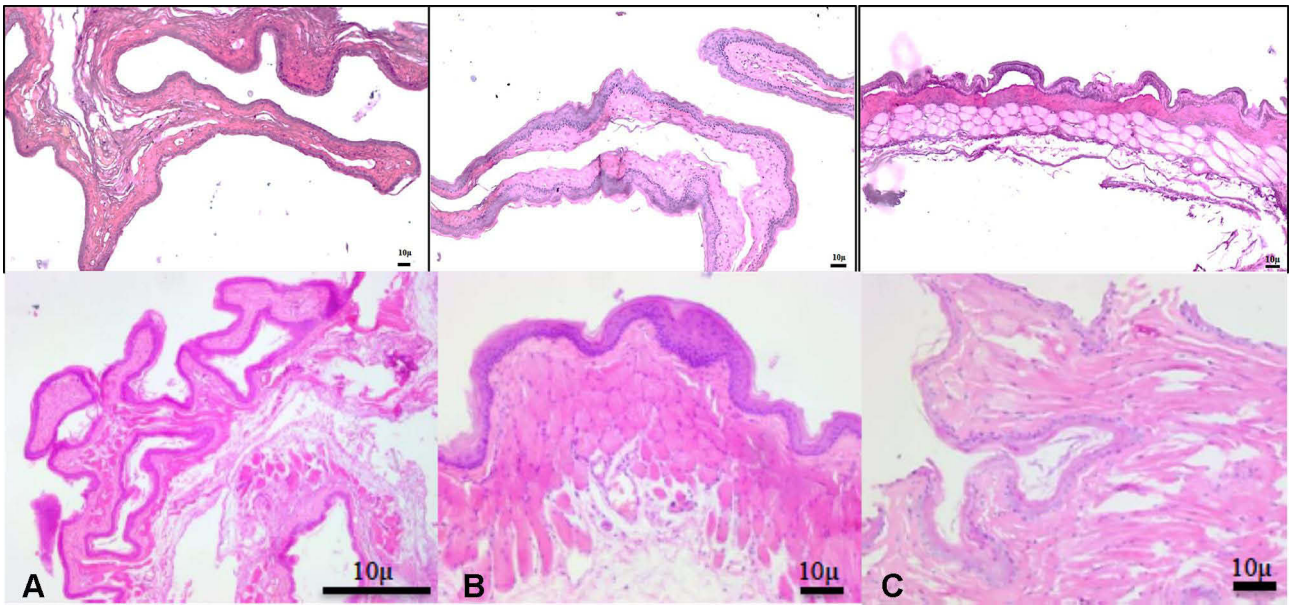

Figure 12 Photomicrographs showing inner buccal mucosa (H&E staining). (**A**) NOHAL solution, (**B**) negative control, (**C**) positive control.

formulation has the potential to be used to inactivate the SARS-CoV-2 in the nose, and the infection may be prevented. The antibacterial effect of NOHAL solution has been proven using strains of *Staphylococcus aureus, Streptococcus pneumoniae* and *Escherichia coli* at specific concentrations and time intervals, and the results of in vitro studies have shown that NOHAL solution reduces viral load as a predictor of anti-viral activity for COVID-19. Cell viability tests have also proven that this antiviral solution does not affect cell

Table 15 Oral Microscopic Irritation Score

Reaction	Numerical Rating							
	1. Subject		2. Subject		3. Subject		Positive Control Subject	
	Left Cheek (Test)	Right Cheek (Negative Control)	Left Cheek (Test)	Right Cheek (Negative Control)	Left Cheek (Test)	Right Cheek (Negative Control)	Left Cheek (Test)	Right Cheek (Negative Control)
Epithelium	0	0	0	0	0	0	3	0
Leukocyte Infiltration (For Every High Penetration Area)	0	0	0	0	0	0	2	0
Vascular Congestion	0	0	0	0	0	0	1	0
Edema	0	0	0	0	0	0	0	0

viability in a toxic way. Skin, oral, nasal and ocular irritation tests using experimental animals did not show any evidence of the irritating effect of NOHAL solution. Therefore, when we considered the concentration and time variations, we found that the effect of the solution showed the strongest antiviral effect when used at 1600 ppm concentration. In the light of the findings obtained from all the experimental steps we have done, it has been predicted that NOHAL solution will reduce and slow down the spread of diseases by acting as a barrier in the transmission of many infectious diseases, particularly COVID-19, in terms of its antimicrobial and antiviral characteristics, without causing damage to neighboring tissues.

Table 16 Nasal Microscopic Irritation Score

Groups	Animal No	Ephitelium	Leukocyte Infiltration (for Every High Penetration Area)	Vascular Congestion	Edema	Irritation Index
Negative Control groups	1	0	0	0	0	0
	2	0	0	0	0	0
	3	0	0	0	0	0
	4	0	0	0	0	0
	5	0	0	0	0	0
	6	0	0	0	0	0
Test Groups	1	0	0	0	0	0
	2	0	0	0	0	0
	3	0	0	0	0	0
	4	0	0	0	0	0
	5	0	0	0	0	0
	6	0	0	0	0	0

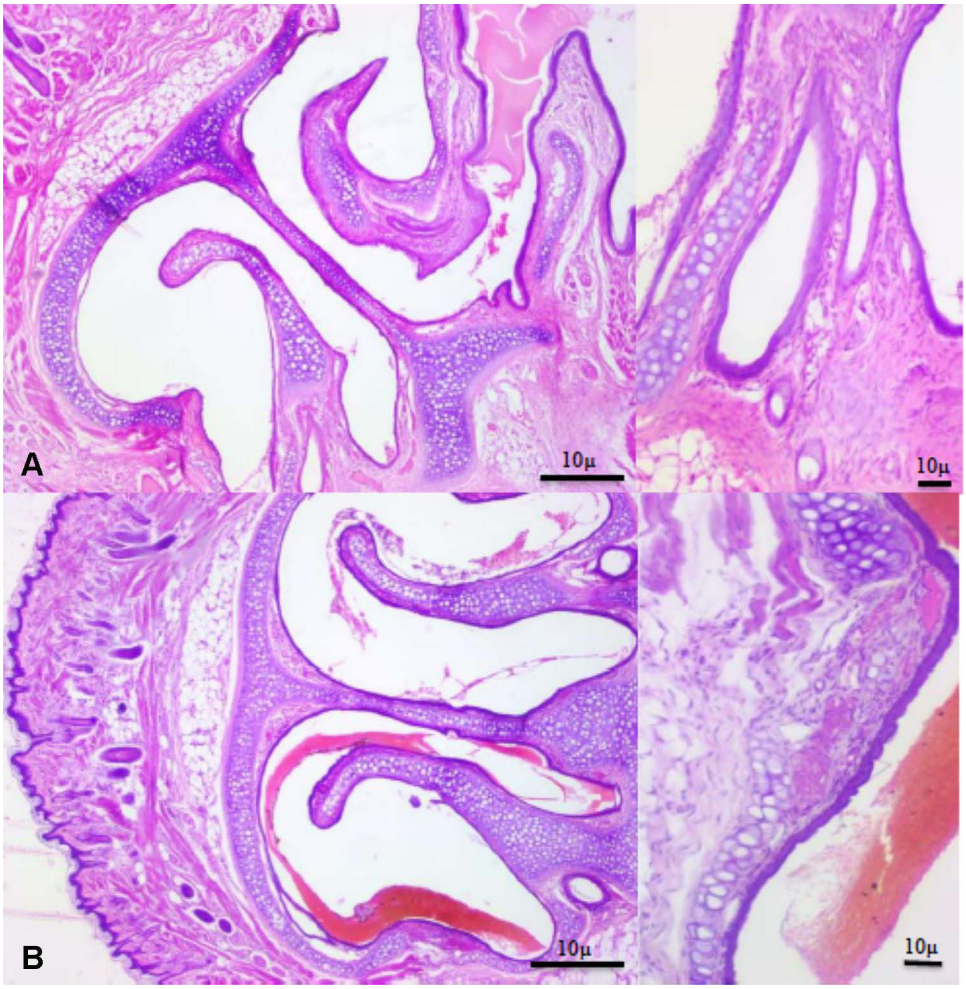

Figure 13 Photomicrographs showing nasal turbinates and nasal mucosa (H&E staining), (**A**) control, (**B**) NOHAL solution.

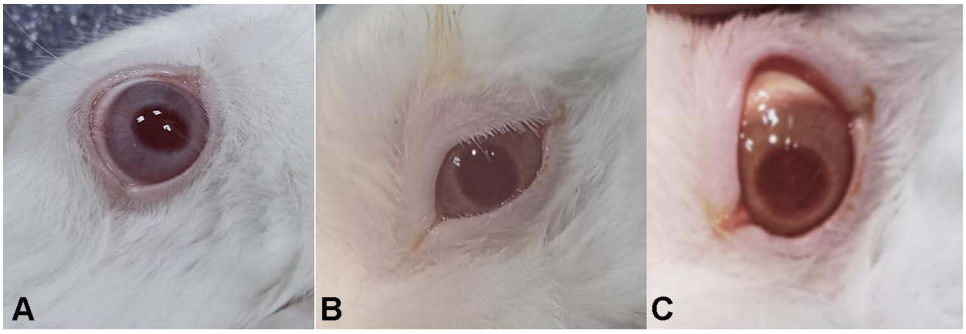

Figure 14 Photos showing ocular irritation test (**A**). Control (right eye), (**B** and **C**) NOHAL solution group (right eye)-fluorescein does not stain a normal cornea, no staining was seen.

Traditional personal protective equipment cannot be replaced by nasal and oral cleansing solutions or gargles. However, those are potential ways of combating SARS-CoV-2 infection as secondary defenses. Furthermore, it is particularly important to support clinical studies in this area rapidly, since clinical trials are the best methods to determine the actual benefits of these agents as well as their role in modifying disease progression and the transmission of SARS-CoV-2.

Table 17 Result of the Ocular Irritation Test

Reaction	Numerical Rating
1.Cornea	0
2.İris	0
3.Conjunctivae	0
Palpebral redness (belonging to the eyelid) and bulbar (belonging to the eyelid) conjunctivae, except cornea and iris	0
Chemosis	0
Fluid discharge	0

Future Directions

The results of future clinical trials will determine the role of NOHAL solution for SARS-CoV-2 mitigation.

Acknowledgments

We express our gratitude to Prof. Necdet Demir, PhD for performing in vivo animal toxicology studies for oral, ocular and intranasal administrations; Prof. Saban Tekin PhD, and Assoc. Prof. Fatma Yücel for guiding us in performing the in vivo challenge test in TUBITAK. Funding was provided by SONOFARMA Pharmaceutical Chemicals Industry and Trade Inc.

Disclosure

Dr. Ahmet Umit SABANCI is the founder of SONOFARMA Pharmaceutical Chemicals Industry and Trade Inc. and has a financial interest in the company. Dr. Ahmet Ümit SABANCI reports a patent WO2019240713A2 pending to World, a patent WO2019240713A3 pending to World, a patent US2021007360A1 pending to USA, a patent TR201904790A pending to Turkey, a patent TR2021-00105 pending to Turkey. The authors report no other conflicts of interest in this work.

References

1. Ratz-lyko A, Arct J, Pytkowska K. Moisturizing and anti-inflammatory properties of cosmetic formulations containing Centella Asiatica extract. *Indian J Pharm Sci*. 2016;78(1):27. doi:10.4103/0250-474X.180247
2. M. Nabil Mawsouf, M.M. El-Sawalhi,G. Martínez-Sánchez, H.A. Darwish,A.A. Shaheen, L. Re. Effect of ozone therapy on redox status in experimentally induced arthritis. *Int J Ozone Ther*. 2010;9(1):7–13.
3. Bocci V. *OZONE a New Medical Drug*. Softcover reprint of hardcover. 1st ed. Springer; 2010.
4. Seyman D, Ozen NS, Inan D, Ongut G, Ogunc D. Pseudomonas aeruginosa septic arthritis of knee after intra-articular ozone injection. *New Microbiol*. 2012;35(3):345–348.
5. Zheng Z, Dong M, Hu K. A preliminary evaluation on the efficacy of ozone therapy in the treatment of COVID-19. *J Med Virol*. 2020;92 (11):2348–2350. doi:10.1002/jmv.26040
6. Rowen RJ, Robins H. Ozone therapy for complex regional pain syndrome: review and case report. *Curr Pain Headache Rep*. 2019;23(6):41. doi:10.1007/s11916-019-0776-y
7. Seydanur Dengizek E, Serkan D, Abubekir E, Aysun Bay K, Onder O, Arife C. Evaluating clinical and laboratory effects of ozone in non-surgical periodontal treatment: a randomized controlled trial. *J Appl Oral Sci*. 2019;27:1–8. doi:10.1590/1678-7757-2018-0108
8. Sconza C, Respizzi S, Virelli L, et al. Oxygen–ozone therapy for the treatment of knee osteoarthritis: a systematic review of randomized controlled trials. *Arthroscopy*. 2020;36(1):277–286. doi:10.1016/j.arthro.2019.05.043
9. Fernández-Cuadros ME. *Ozone Fundamentals and Effectiveness on Knee Pain: Chondromalacia and Knee Osteoarthritis*. LAP LAMBERT Academic Publishing; 2016.
10. Fernández-Cuadros ME, Pérez-Moro OS, Albaladejo-Florin MJ, Alava-Rabasa S. El ozono intraarticular modula la inflamación, mejora el dolor, la rigidez, la función y tiene un efecto anabólico sobre la artrosis de rodilla: estudio cuasi-experimental prospectivo tipo antes-después, 115 pacientes. *Revista de La Sociedad Española Del Dolor*. 2020;27:78–86. doi:10.20986/resed.2020.3775/2019
11. Alkan PE, Güneş M, Özakin C, Sabanci A. New antibacterial agent: nanobubble ozone stored in liposomes: the antibacterial activity of nanobubble ozone in liposomes and their thymol solutions. *Ozone Sci Eng*. 2021;1–5. doi:10.1080/01919512.2021.1904205
12. Monzillo V, Lallitto F, Russo A, et al. Ozonized gel against four candida species: a pilot study and clinical perspectives. *Materials*. 2020;13(7):1731. doi:10.3390/ma13071731
13. Jakab GJ, Hmieleski RR. Reduction of influenza virus pathogenesis by exposure to 0.5 ppm ozone. *J Toxicol Environ Health*. 1988;23 (4):455–472. doi:10.1080/15287398809531128
14. Finch GR, Black EK, Labatiuk CW, Gyürék L, Belosevic M. Comparison of Giardia lamblia and Giardia muris cyst inactivation by ozone. *Appl Environ Microbiol*. 1993;59(11):3674–3680. doi:10.1128/aem.59.11.3674-3680.1993
15. Criegee R. Mechanism of Ozonolysis. *Angew Chem Int Ed Engl*. 1975;14(11):745–752. doi:10.1002/anie.197507451
16. Song M, Zeng Q, Xiang Y, et al. The antibacterial effect of topical ozone on the treatment of MRSA skin infection. *Mol Med Rep*. 2017;17:2449–2455. doi:10.3892/mmr.2017.8148
17. Russo T, Currò M, Ferlazzo N, et al. Stable ozonides with vitamin E acetate versus corticosteroid in the treatment of lichen sclerosus in foreskin: evaluation of effects on inflammation. *Urol Int*. 2019;103 (4):459–465. doi:10.1159/000499846
18. Xiao W, Tang H, Wu M, et al. Ozone oil promotes wound healing by increasing the migration of fibroblasts via PI3K/Akt/mTOR signaling pathway. *Biosci Rep*. 2017;37(6):1–9. doi:10.1042/BSR20170658
19. Murata T, Komoto S, Iwahori S, et al. Reduction of severe acute respiratory syndrome coronavirus-2 infectivity by admissible concentration of ozone gas and water. *Microbiol Immunol*. 2020;65(1):10–16. doi:10.1111/1348-0421.12861
20. Franzini M, Valdenassi L, Ricevuti G, et al. Oxygen-ozone (O2-O3) immunoceutical therapy for patients with COVID-19. Preliminary evidence reported. *Int Immunopharmacol*. 2020;88:106879. doi:10.1016/j.intimp.2020.106879
21. Hernández A, Viñals M, Pablos A, et al. Ozone therapy for patients with COVID-19 pneumonia: preliminary report of a prospective case-control study. *Int Immunopharmacol*. 2021;90:107261. doi:10.1016/j.intimp.2020.107261

22. Tascini C, Sermann G, Pagotto A, et al. Blood ozonization in patients with mild to moderate COVID-19 pneumonia: a single centre experience. *Intern Emerg Med*. 2020;16(3):669–675. doi:10.1007/s11739-020-02542-6
23. Fernández-Cuadros ME, Albaladejo-Florín MJ, Álava-rabasa S, et al. Effect of rectal ozone (O3) in severe COVID-19 pneumonia: preliminary results. *SN Compr Clin Med*. 2020;2(9):1328–1336. doi:10.1007/s42399-020-00374-1
24. Bateman RM, Sharpe MD, Ellis CG. Bench-to-bedside review: microvascular dysfunction in sepsis – hemodynamics, oxygen transport, and nitric oxide. *Crit Care*. 2003;7(5):359–373. doi:10.1186/cc2353
25. Giunta R, Coppola A, Luongo C, et al. Ozonized autohemotransfusion improves hemorheological parameters and oxygen delivery to tissues in patients with peripheral occlusive arterial disease. *Ann Hematol*. 2001;80:745–748. doi:10.1007/s002770100377
26. Wu XN, Zhang T, Wang J, et al. Magnetic resonance diffusion tensor imaging following major ozonated autohemotherapy for treatment of acute cerebral infarction. *Neural Regen Res*. 2016;11(7):1115–1121. doi:10.4103/1673-5374.187046
27. Borroto RV, Lima HLB, Lima GS, et al. Prevention of the stroke with the application of ozone therapy. *Rev Cub Med Fis Rehab*. 2013;5(1):3–16.
28. Pandolfi S, Zammitti A, Franzini M, et al. Effects of oxygen ozone therapy on cardiac function in a patient with a prior myocardial infarction. *Ozone Ther*. 2017;2(1). doi:10.4081/ozone.2017.6745
29. Clavo B, Suarez G, Aguilar Y, et al. Brain ischemia and hypometabolism treated by ozone therapy. *Forsch Komplementmed*. 2011;18(5):283–287. doi:10.1159/000333795
30. Kekez MM, Sattar SA. A new ozone-based method for virus inactivation: preliminary study. *Phys Med Biol*. 1997;42:2027–2039. doi:10.1088/0031-9155/42/11/002
31. Shin GA, Sobsey MD. Reduction of Norwalk virus, poliovirus 1, and bacteriophage MS2 by ozone disinfection of water. *Appl Environ Microbiol*. 2003;69:3975–3978. doi:10.1128/AEM.69.7.3975-3978.2003
32. Herbold K, Flehmig B, Botzenhart K. Comparison of ozone inactivation, in flowing water, of hepatitis A virus, poliovirus 1, and indicator organisms. *Appl Environ Microbiol*. 1989;55:2949–2953. doi:10.1128/aem.55.11.2949-2953.1989
33. Katzenelson E, Koerner G, Biedermann N, Peleg M, Shuval HI. Measurement of the inactivation kinetics of polio virus by ozone in a fast-flow mixer. *Appl Environ Microbiol*. 1979;37:715–718. doi:10.1128/aem.37.4.715-718.1979
34. Roy D, Wong PK, Engelbrecht RS, Chian ES. Mechanism of enteroviral inactivation by ozone. *Appl Environ Microbiol*. 1981;41:718–723. doi:10.1128/aem.41.3.718-723.1981
35. Rowen RJ, Robins H. A plausible "Penny" costing effective treatment for corona virus - ozone therapy. *J Infect Dis Epidemiol*. 2020;6(2):1–5.
36. Mirazimi A, Mousavi-Jazi M, Sundqvist VA, Svensson L. Free thiol groups are essential for infectivity of human cytomegalovirus. *J Gen Virol*. 1999;80:2861–2865. doi:10.1099/0022-1317-80-11-2861
37. Markovic I, Stantchev TS, Fields KH, et al. Thiol/disulfide exchange is a prerequisite for CXCR4-tropic HIV-1 envelope-mediated T-cell fusion during viral entry. *Blood*. 2004;103:1586–1594. doi:10.1182/blood-2003-05-1390
38. Lee JE, Saphire EO. Ebolavirus glycoprotein structure and mechanism of entry. *Future Virol*. 2009;4:621–635. doi:10.2217/fvl.09.56
39. Madu IG, Belouzard S, Whittaker GR. SARS-coronavirus spike S2 domain flanked by cysteine residues C822 and C833 is important for activation of membrane fusion. *Virology*. 2009;393(2):265–271. doi:10.1016/j.virol.2009.07.038
40. Pandey A, Nikam AN, Mutalik SP, et al. Architectured therapeutic and diagnostic nanoplatforms for combating SARS-CoV-2: role of inorganic, organic, and radioactive materials. *ACS Biomater Sci Eng*. 2020;7(1):31–54. doi:10.1021/acsbiomaterials.0c01243
41. Koo H, Huh MS, Sun IC, et al. In vivo targeted delivery of nanoparticles for theranosis. *Acc Chem Res*. 2011;44(10):1018–1028. doi:10.1021/ar2000138
42. Abo-zeid Y, Urbanowicz RA, Thomson BJ, Irving WL, Tarr AW, Garnett MC. Enhanced nanoparticle uptake into virus infected cells: could nanoparticles be useful in antiviral therapy? *Int J Pharm*. 2018;547(1–2):572–581. doi:10.1016/j.ijpharm.2018.06.027
43. Clinical and Laboratory Standards Institute. *Methods for Dilution Antimicrobial Susceptibility Tests for Bacteria That Grow Aerobically*. CLSI standart M07. 11th ed. Wayne,PA: Clinical and Laboratory Standards Institute; 2018.
44. Xie X, Muruato A, Lokugamage KG, et al. An infectious cDNA clone of SARS-CoV-2. *Cell Host Microbe*. 2020;27(5):841–848.e3. doi:10.1016/j.chom.2020.04.004
45. Alkan PE, Güneş ME, Özakin C, Sabanci AÜ. New antibacterial agent: nanobubble ozone stored in liposomes: the antibacterial activity of nanobubble ozone in liposomes and their thymol solutions. *Ozone Sci Eng*. 2021;43(6):637–641. doi:10.1080/01919512.2021.1904205
46. Erkan-Alkan P, Güneş ME, Özakın C, Sabancı AÜ. [Nanoparticle liposomes: a new strategy in bacterial infections]. *Klimik Derg*. 2021;34(2):99–102. Turkish. doi:10.36519/kd.2021.3633
47. Borges GÁ, Elias ST, da Silva SM, et al. *In vitro* evaluation of wound healing and antimicrobial potential of ozone therapy. *Journal of Cranio-Maxillofacial Surgery*. 2017;45(3):364–370. doi:10.1016/j.jcms.2017.01.005
48. Clavo B, Córdoba-Lanús E, Rodríguez-Esparragón F, et al. Effects of ozone treatment on personal protective equipment contaminated with SARS-CoV-2. *Antioxidants*. 2020;9:1222. doi:10.3390/antiox9121222
49. Zhu N, Zhang D, Wang W, et al. A novel coronavirus from patients with pneumonia in China, 2019. *N Engl J Med*. 2020;382(8):727–733. doi:10.1056/NEJMoa2001017
50. Mao P, Wu S, Li J, et al. Human alveolar epithelial type II cells in primary culture. *Physiol Rep*. 2015;3(2):e12288. doi:10.14814/phy2.12288
51. Fulcher ML, Randell SH. Human nasal and tracheo-bronchial respiratory epithelial cell culture. *Methods Mol Biol*. 2013;945:109–121.
52. Stevens A, Wilson I. The haematoxylins and eosin. In: Bancroft JD, Stevens A, editors. *Theory and Practice of Histological Techniques*. 4th ed. Hong Kong: Churchill Livingstone; 1999:99–112.
53. Yoon JG, Yoon J, Song JY, et al. Clinical significance of a high SARS-CoV-2 viral load in the saliva. *J Korean Med Sci*. 2020;35(20):1–5. doi:10.3346/jkms.2020.35.e195
54. Zou L, Ruan F, Huang M, et al. SARS-CoV-2 viral load in upper respiratory specimens of infected patients. *N Engl J Med*. 2020;382(12):1177–1179. doi:10.1056/NEJMc2001737
55. Zhou P, Yang XL, Wang XG, et al. A pneumonia outbreak associated with a new coronavirus of probable bat origin. *Nature*. 2020;579:270–273. doi:10.1038/s41586-020-2012-7
56. Li W, Moore MJ, Vasilieva N, et al. Angiotensin-converting enzyme 2 is a functional receptor for the SARS coronavirus. *Nature*. 2003;426:450–454. doi:10.1038/nature02145
57. Hoffmann M, Kleine-Weber H, Schroeder S, et al. SARS-CoV-2 cell entry depends on ACE2 and TMPRSS2 and is blocked by a clinically proven protease inhibitor. *Cell*. 2020;181:271–280.e8. doi:10.1016/j.cell.2020.02.052
58. Matsuyama S, et al. Efficient activation of the severe acute respiratory syndrome coronavirus spike protein by the transmembrane protease TMPRSS2. *J Virol*. 2010;84:12658–12664. doi:10.1128/JVI.01542-10
59. Iwata-Yoshikawa N, Okamura T, Shimizu Y, Hasegawa H, Takeda M, Nagata N. TMPRSS2 contributes to virus spread and immunopathology in the airways of murine models after coronavirus infection. *J Virol*. 2019;93. doi:10.1128/JVI.01815-18

60. Sungnak W, Huang N, Bécavin C, et al. SARS-CoV-2 entry factors are highly expressed in nasal epithelial cells together with innate immune genes. *Nat Med*. 2020;26:681–687. doi:10.1038/s41591-020-0868-6
61. Zhong M, Lin B, Pathak JL, et al. ACE2 and furin expressions in oral epithelial cells possibly facilitate COVID-19 infection via respiratory and fecal-oral routes. *Front Med*. 2020;7:580796. doi:10.3389/fmed.2020.580796
62. Singapore Standards Council. *Standard Guide for Accelerated Aging of Sterile Barrier Systems for Medical Devices*. Enterprise Singapore; 2020.
63. He X, Lau EHY, Wu P, et al. Temporal dynamics in viral shedding and transmissibility of COVID-19. *Nat Med*. 2020;26(5):672–675. doi:10.1038/s41591-020-0869-5
64. Ramalingam S, Graham C, Dove J, Morrice L, Sheikh A. A pilot, open labelled, randomised controlled trial of hypertonic saline nasal irrigation and gargling for the common cold. *Sci Rep*. 2019;9(1):1–9. doi:10.1038/s41598-018-37703-3
65. Rabago D, Zgierska A. Saline nasal irrigation for upper respiratory conditions. *Am Fam Phys*. 2009;80(10):1117–1119.
66. Chatterjee U, Chakraborty A, Naskar S, Saha B, Bandyapadhyay B, Shee S. Efficacy of normal saline nasal spray and gargle on SARS-CoV-2 for prevention of COVID-19 pneumonia. *Res Sq*. 2021;1–7. doi:10.21203/rs.3.rs-153598/v2
67. Ludwig M, Enzenhofer E, Schneider S, et al. Efficacy of a Carrageenan nasal spray in patients with common cold: a randomized controlled trial. *Respir Res*. 2013;14(1):124. doi:10.1186/1465-9921-14-124
68. Giarratana N, Rajan B, Kamala K, Mendenhall M, Reiner G. A sprayable acid-oxidizing solution containing hypochlorous acid (AOS2020) efficiently and safely inactivates SARS-Cov-2: a new potential solution for upper respiratory tract hygiene. *Eur Arch Otorhinolaryngol*. 2021:1–5. doi:10.1007/s00405-020-06112-6
69. Shmuel K, Dalia M, Tair L, Yaakov N. Low pH Hypromellose (Taffix) nasal powder spray could reduce SARS-CoV-2 infection rate post mass-gathering event at a highly endemic community: an observational prospective open label user survey. *Expert Rev Anti Infect Ther*. 2021;19:1325–1330.
70. Anderson DE, Sivalingam V, Kang AEZ, et al. Povidone-iodine demonstrates rapid in vitro virucidal activity against SARS-CoV-2, the virus causing COVID-19 disease. *Infect Dis Ther*. 2020;9(3):669–675. doi:10.1007/s40121-020-00316-3
71. PVP-I nasal sprays and SARS-CoV-2 nasopharyngeal titers (for COVID-19) - full text view - ClinicalTrials.gov. Clinical Trials; 2021.
72. Braga SS. Cyclodextrins: emerging medicines of the new millennium. *Biomolecules*. 2019;9(12):801. doi:10.3390/biom9120801
73. Ergoren MC, Paolacci S, Manara E, et al. A pilot study on the preventative potential of alpha-cyclodextrin and hydroxytyrosol against SARS-CoV-2 transmission. *Acta Biomed*. 2020;91(Supplement 13):e2020022. doi:10.23750/abm.v91i13-S.10817
74. Carrouel F, Gonçalves L, Conte M, et al. Antiviral activity of reagents in mouth rinses against SARS-CoV-2. *J Dent Res*. 2020;100(2):124–132. doi:10.1177/0022034520967933
75. Altaş B, Koçak H, Sltınay S, Yücabaş K, Taşkın M, Oktay F. Is ozone (O3) treatment effective in atrophic rhinitis: experimental animal study. *Otolaryngol Polska*. 2018;72(5):37–44. doi:10.5604/01.3001.0012.1265
76. Shah M, Captain J, Vaidya V, et al. Safety and efficacy of ozone therapy in mild to moderate COVID-19 patients: a phase 1/11 randomized control trial (SEOT study). *Int Immunopharmacol*. 2021;91:107301. doi:10.1016/j.intimp.2020.107301
77. Cattel F, Giordano S, Bertiond C, et al. Ozone therapy in COVID-19: a narrative review. *Virus Res*. 2021;291:198207. doi:10.1016/j.virusres.2020.198207
78. Tizaoui C. Ozone: a potential oxidant for COVID-19 virus (SARSCoV-2). *Ozone Sci Eng*. 2020;42(5):378–385. doi:10.1080/01919512.2020.1795614
79. Casale M, Moffa A, Sabatino L, et al. Hyaluronic acid: perspectives in upper aero-digestive tract. A systematic review. *PLoS One*. 2015;10(6):e0130637. doi:10.1371/journal.pone.0130637
80. Mösges R, Baena-Cagnani CE, Passali D. Nonpharmacological treatment of rhinoconjunctivitis and rhinosinusitis. *J Allergy*. 2014;(2014:1–2. doi:10.1155/2014/416236
81. El Kechai N, Geiger S, Fallacara A, et al. Mixtures of hyaluronic acid and liposomes for drug delivery: phase behavior, microstructure and mobility of liposomes. *Int J Pharm*. 2017;523(1):246–259. doi:10.1016/j.ijpharm.2017.03.029
82. Arpicco S, Lerda C, Dalla Pozza E, et al. Hyaluronic acid-coated liposomes for active targeting of gemcitabine. hyaluronic acid-coated liposomes for active targeting of gemcitabine. *Eur J Pharm Biopharm*. 2013;85:373–380. doi:10.1016/j.ejpb.2013.06.003
83. Danaei M, Dehghankhold M, Ataei S, et al. Impact of particle size and polydispersity index on the clinical applications of lipidic nanocarrier systems. *Pharmaceutics*. 2018;10:57. doi:10.3390/pharmaceutics10020057
84. Schreiner TB, Santamaria-Echart A, Ribeiro A, et al. Formulation and optimization of nanoemulsions using the natural surfactant saponin from quillaja bark. *Molecules*. 2020b;25(7):1538. doi:10.3390/molecules25071538
85. Creech, C. B., Walker, S. C., & Samuels, R. J. SARS-CoV-2 Vaccines. JAMA, 2021; 325(13), 1318. doi:10.1001/jama.2021.3199